

Paleomagnetic constraints on the Mesozoic-Cenozoic paleolatitudinal and rotational history of Indochina and South China: Review and updated kinematic reconstruction



Shihu Li^{a,*}, Eldert L. Advokaat^b, Douwe J.J. van Hinsbergen^b, Mathijs Koymans^b,
Chenglong Deng^a, Rixiang Zhu^a

^a State Key Laboratory of Lithospheric Evolution, Institute of Geology and Geophysics, Chinese Academy of Sciences, Beijing 100029, China

^b Department of Earth Sciences, Utrecht University, Budapestlaan 17, 3584 CD Utrecht, The Netherlands

ARTICLE INFO

Keywords:

Extrusion
Rotation
Indochina Block
Tibetan Plateau
Paleomagnetic

ABSTRACT

Paleomagnetic data have long been used to hypothesize that the Cenozoic extrusion of the Indochina Block along the left-lateral Ailao Shan-Red River fault, as a result of the India-Asia collision, may have been associated with a major southward paleolatitude shift of as much as 10–15°, and a vertical-axis rotation of as much as 25–40°. However, although numerous paleomagnetic studies have been conducted in the southeast margin of the Tibetan Plateau and in the Indochina region during the last few decades, the detailed rotation as well as the latitudinal displacement of the Indochina Block remain controversial because of apparently contradicting paleomagnetic results. Geological constraints also yield contrasting estimates on the amount of displacement along different segment of the Ailao Shan-Red River fault: 700 ± 200 km in the northwest, but only ~250 km in the southeast. In this paper, the available paleomagnetic data from the southeast margin of the Tibetan Plateau and Indochina, as well as the South China Block, from Jurassic and younger rocks are compiled and critically reviewed using the new paleomagnetic toolkit on Paleomagnetism.org. Our results show that (1) the South China Block has declinations that reveal no significant rotations relative to Eurasia since latest Jurassic. Inclinations are consistently shallower than expected, which is likely the result of inclination shallowing in sedimentary rocks; (2) there is no paleomagnetically resolvable southward motion of the Indochina Block with respect to Eurasia based on the paleomagnetic data. Paleomagnetic inclinations are in fact lower than expected, probably due to inclination shallowing in sediments; (3) paleomagnetic declinations reveal large, more or less coherently rotating blocks in the northern Indochina domain and the SE Tibetan margin that rotated up to 70° clockwise, much more than the ~10–15° rotation of the stable, SE part of the Indochina Block. These blocks are bounded by fold-thrust belts and strike-slip faults, which we interpret to have accommodated these block rotations during the Cenozoic. We designed a new tool on the online open-access portal Paleomagnetism.org that allows testing whether Euler rotations in a kinematic reconstruction fulfill paleomagnetic data. Using this tool, we built a first-order kinematic reconstruction of rotational deformation of northwest Indochina in Cenozoic. We show that the northwestern part of Indochina extruded 350 km more along the Ailao Shan-Red River fault than the southeastern part accommodated by internal northwest Indochina rotation and deformation. Estimates of 250 km of extrusion of the southeastern part of the Indochina then predicts ~600 km of left-lateral motion along the northwestern part of the Ailao Shan-Red River fault, which reconciles the small and large estimates that prevail in the literature of extrusion of Indochina from the Tibetan realm during the Cenozoic India-Asia collision.

1. Introduction

The Tibetan Plateau, the largest and highest continental plateau in the world, is the product of convergence between the Indian and Eurasian plates, and the collision of the Indian and Eurasian continental

crusts since the Early Cenozoic (see review in [Hu et al., 2016](#)). This collision has not only led to the formation of the Himalaya orogenic belt, and major shortening in the Tibetan Plateau as well as in central Asia to the north ([Molnar and Tapponnier, 1975](#)), but was also associated with extrusion of Indochina along the Ailao Shan-Red River

* Corresponding author.

E-mail address: lsh917@mail.iggcas.ac.cn (S. Li).

<http://dx.doi.org/10.1016/j.earscirev.2017.05.007>

Received 18 January 2017; Received in revised form 9 May 2017; Accepted 16 May 2017

Available online 18 May 2017

0012-8252/ © 2017 Elsevier B.V. All rights reserved.

fault in the east, and the Shan Scarp-Sagaing fault in the west (Tapponnier et al., 1982; Leloup et al., 1995; Bertrand et al., 2001; Replumaz and Tapponnier, 2003; van Hinsbergen et al., 2011a). A long-lasting kinematic problem in the tectonic evolution of the Tibetan Plateau is how and where the crustal deformation accommodated the major plate convergence between India and Eurasia since collision. The age of collision is debated, ranging from as old as ~70 Ma to as young as ~34 Ma (e.g., Hu et al., 2016), but is widely accepted to be between 60 and 50 Ma based on arrival of Asian sediments in Tibetan Himalayan stratigraphy (e.g., Orme et al., 2014; Hu et al., 2015, 2016), the onset of Tibetan Himalayan high-pressure metamorphism (e.g., Leech et al., 2005), and paleomagnetism (e.g., Dupont-Nivet et al., 2010; Najman et al., 2010; Sun et al., 2010; Yi et al., 2011; Lippert et al., 2014; Ma et al., 2014). An alternative proposal suggests that this collision reflects emplacement of ophiolites that are widespread in the suture instead (e.g., Aitchison et al., 2007; Jagoutz et al., 2015), but these ophiolites were paleomagnetically shown to have formed adjacent to Lhasa, and are unconformably overlain and underthrust by Cretaceous, Lhasa-derived clastic sedimentary rocks (e.g., Orme et al., 2014, Huang et al., 2015). A 50–60 Ma collision age shows an amount of post-collisional India-Asia convergence, constrained by Indo-Atlantic ocean basin reconstructions, of ~3000 to 5000 km (Molnar and Stock, 2009; Copley et al., 2010; van Hinsbergen et al., 2011b, 2012).

Tapponnier et al. (1982) recognized that not only N-S shortening played a role in accommodating N-S India-Eurasia convergence in Tibet, but that also major strike-slip faults had developed, including the left-lateral Ailao Shan-Red River fault (Fig. 1), along which crust has been extruded from the collision zone. Since that time, several views

have been put forward based on disparate estimates on the amount of displacement along the Ailao Shan-Red River fault (Fig. 2). While there is agreement on major displacements, estimates vary from as low as ~250 km, to ~700 km or as large as 1200–1500 km (Leloup et al., 1995), and associated clockwise rotations are predicted to be anywhere between a few degrees and 40° (Tapponnier et al., 1982, 1990, 2001; Lee and Lawver, 1995; Leloup et al., 1995; Wang and Burchfiel, 1997; Hall, 2002; Replumaz and Tapponnier, 2003; Searle, 2006; Royden et al., 2008; Fyhn et al., 2009; van Hinsbergen et al., 2011a). The low end-member of the displacement estimates has been taken to suggest that Indochina extrusion plays only a modest role in accommodating India-Eurasia convergence (e.g., Hall, 2002; Searle, 2006; van Hinsbergen et al., 2011a), whereas the high end-member suggests that Indochina was originally located north of the Himalaya and its extrusion was a prime mechanism accommodating post-collisional convergence (Tapponnier et al., 1982, 1990, 2001; Lee and Lawver, 1995; Leloup et al., 1995; Replumaz and Tapponnier, 2003; Royden et al., 2008; Ingalls et al., 2016). The two schools of thought in addition predict very different amounts of paleolatitudinal motion of Indochina relative to the South China Block, and of clockwise rotation of Indochina in the Cenozoic.

Paleomagnetism provides a direct quantitative tool to constrain latitudinal motion and vertical axis rotation, and consequently a large paleomagnetic database of Indochina and South China has been acquired over the last decades (Otofujii et al., 1990, 1998, 2010, 2012; Funahara et al., 1992, 1993; Huang and Opdyke, 1992, 1993, 2015; Yang and Besse, 1993; Yang et al., 1995, 2001a, b; Richter and Fuller, 1996; Sato et al., 1999, 2001, 2007; Yoshioka et al., 2003; Tamai

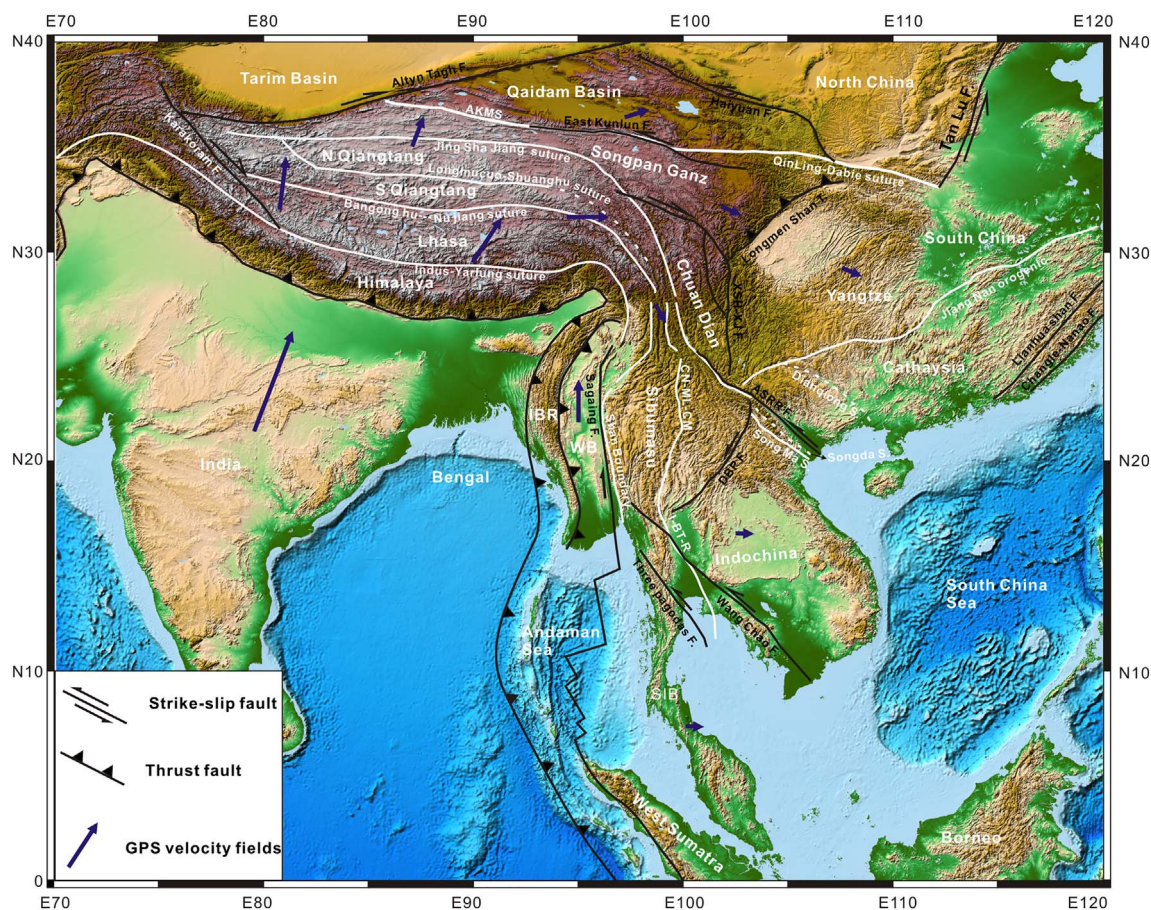


Fig. 1. Simplified geological map showing the main tectonic units of Southeast Asia. The white and black lines represent major sutures and faults, respectively. The GPS velocity fields showing relative motions of SE Asia with respect to Eurasia are from Vigny et al. (2003) and Gan et al. (2007). Abbreviations: AKMS: Anyimaqin-Kunlun-Muztagh suture, ASRRF: Ailao Shan-Red River fault, CN-ML-CM: Changning-Menglian-Chiang Mai suture, I-BT-R: Inthanon-Bentong-Raub suture, DBPF: Dien Bien Phu fault, IBR: Indo-Burma Ranges, SIB: Sibumasu Block, WB: West Burma Block.

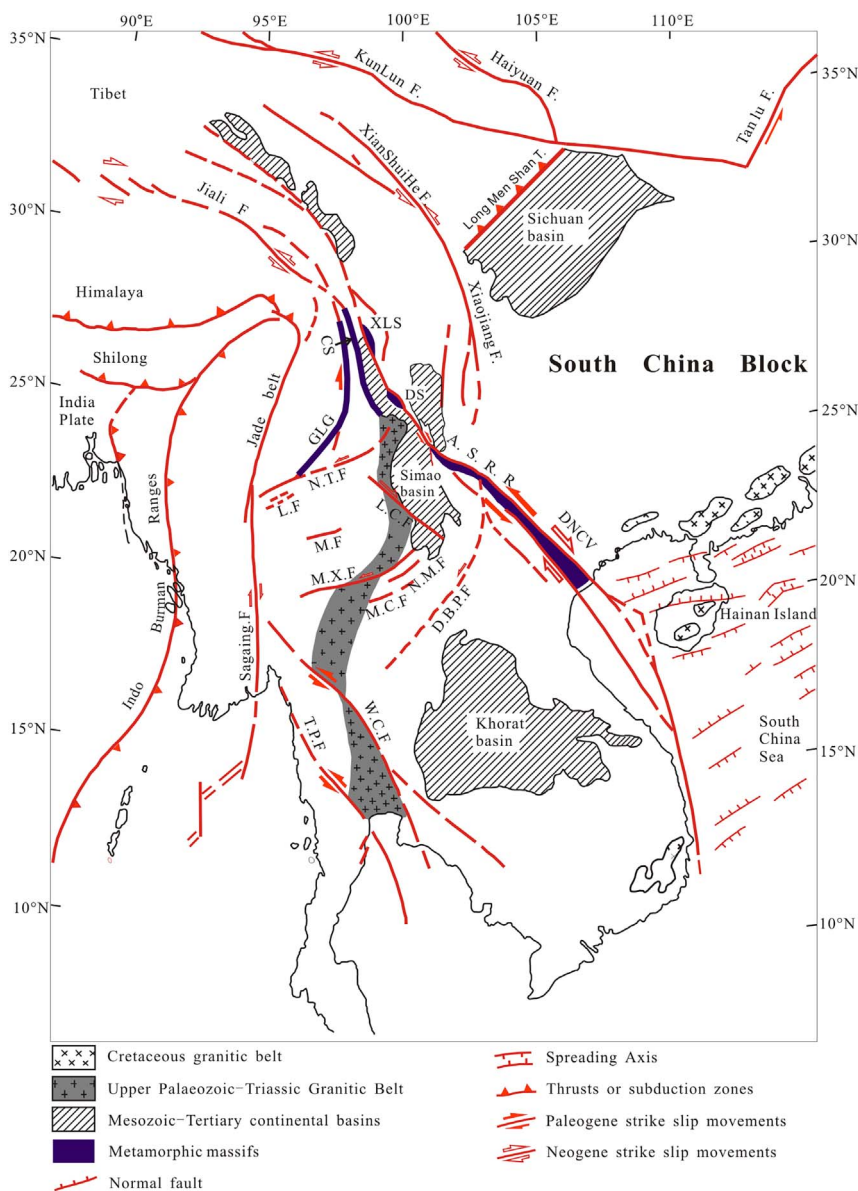


Fig. 2. Detailed tectonic map of the southeast margin of Tibetan Plateau, modified after [Leloup et al. \(1995\)](#). A.S.R.R.: Ailao Shan-Red River shear zone, CS: Chongshan shear zone, DS: Diancang Shan Shear Zone, DNCV: Day Nui Con Voi Shear Zone, GIG: Gaoligong shear zone, XLS: Xuelong Shan Shear Zone. D.B.P.F.: Dien Bien Phu fault, L.C.F.: Lancang fault, L.F.: Lashio fault, M.C.F.: Mae Chan fault, M.F.: Menglian fault, M.X.F.: Mengxing fault, N.M.F.: Nam Ma fault, N.T.F.: Nanting River fault, T.P.F.: Three Pagodas fault, W.C.F.: Wang Chao fault.

et al., 2004; Takemoto et al., 2005, 2009; Charusiri et al., 2006; Aihara et al., 2007; Tanaka et al., 2008; Kondo et al., 2012; Li et al., 2012, 2013a; Chi and Geissman, 2013; Tong et al., 2013, 2015, 2016; Fujiwara et al., 2014; Kornfeld et al., 2014a, b; Gao et al., 2015; Wang et al., 2016). [Achache et al. \(1983\)](#) is the first to review the available Cretaceous and Cenozoic paleomagnetic data from Southeast Asia to test the amount of latitudinal motion and rotation of the Indochina Block, and they argued that the Indochina Block experienced a $24 \pm 12^\circ$ clockwise rotation and a $4.6 \pm 7.6^\circ$ ($\sim 500 \pm 1280$ km) southward motion relative to the Eurasia after the Middle Jurassic. Since then, a large number of paleomagnetic studies followed, which did not provide a unified, but a rather conflicting view on deformation in Indochina: paleomagnetic declinations range from $\sim 120^\circ$ clockwise rotation to no significant rotation (e.g., [Yang and Besse, 1993](#); [Chen et al., 1995](#); [Yang et al., 1995](#); [Li et al., 2012](#); [Chi and Geissman, 2013](#); [Tong et al., 2013](#)), while the proposed latitudinal displacement based on paleomagnetic inclinations varies from as much as 1500 km southward motion in the Cenozoic to even northward motion relative to South China (see review in [van Hinsbergen et al., 2011a](#)). The rotation

results suggest that the Indochina region between the Ailao Shan-Red River fault and the Shan Scarp-Sagaing fault is not occupied by a single, rigid block, but that the region suffered internal deformations and vertical axis block rotations ([Aihara et al., 2007](#); [Sato et al., 2001, 2007](#); [Tanaka et al., 2008](#); [Yang et al., 2001b](#); [Kondo et al., 2012](#); [Tong et al., 2013](#)). The reasons for this discrepancy may be several. First, in such a large paleomagnetic dataset, there may be a large variation in quality and reliability of the data, for instance, owing to major differences in the amount of data per study. A few old datasets were not subjected to complete demagnetization (e.g., [Maranate and Vella, 1986](#)) and some of the data are probably remagnetized ([Chen et al., 1995](#); [Yamashita et al., 2011](#); [Kornfeld et al., 2014a](#); [Huang and Opdyke, 2015](#); [Tsuchiyama et al., 2016](#); [Li et al., 2017](#)). Second, some of the paleomagnetically-detected rotations may reflect localized deformation instead of a rigid block rotation in such a tectonically active region (e.g., [Yang et al., 2001b](#); [Tong et al., 2013](#)). Third, most of these paleomagnetic data were derived from Mesozoic rocks, and the scarcity of Cenozoic paleomagnetic data prevents us from better understanding the rotation and latitudinal displacement of the Indochina Block during

the Cenozoic deformation of Tibetan Plateau. Last, most of, if not all, paleomagnetic studies were conducted on sedimentary red beds, which generally shows a strong tendency to inclination shallowing due to compaction that results in erroneous paleolatitude estimates (e.g., King, 1955; Tan et al., 2003; Tauxe, 2005; Kodama, 2012). Some studies from the South China Block (Narumoto et al., 2006; Sun et al., 2006; Wang and Yang, 2007; Li et al., 2013b) and Indochina (Li et al., 2013a; Tong et al., 2013, 2015) took these effects into account, but most of the previous studies did not address this problem. Therefore, a critical assessment and review of these data is timely.

Recently, an online paleomagnetic toolset has become available that allows for an efficient integration of major paleomagnetic datasets (www.paleomagnetism.org, Koymans et al., 2016). In this paper, we use this toolset to review and integrate the extensive paleomagnetic dataset (177 individual sites) obtained from Jurassic and younger rocks of Indochina, the southeastern Tibetan Plateau, and the South China Block. We will use this integrated dataset to critically assess the tectonic conclusions drawn on the extrusion of Indochina as a whole. To this end, we review the structural and stratigraphic constraints on deformation within the Indochina region and then build the paleomagnetic database. We will discuss the role of well-known paleomagnetic artifacts, such as inclination shallowing, in previous paleolatitudinal motion estimates, and provide an improved kinematic restoration of the internal deformation that occurred within the larger Indochina region since the Early Cenozoic that for the first time reconciles structural and paleomagnetic constraints.

2. Geological setting

2.1. Tectonic framework

SE Asia comprises a complex collage of continental fragments separated by Paleozoic to Cenozoic sutures where oceanic basins were consumed. These include the blocks of North China, South China, Indochina, Sibumasu, and West Burma in the east, and the continent-derived rocks of the Tethys Himalaya, Lhasa, Qiangtang, and the Northeast Tibetan terranes as well as the Songpan-Ganzi flysch belt, together forming the Tibetan Plateau in the west (Fig. 1). All of these continental blocks are interpreted as derived from Gondwana since the Early Paleozoic (e.g., Metcalfe, 2013). They separated from Gondwana, drifted to the north and eventually accreted to North China and Siberia throughout the Paleozoic and Mesozoic, associated with the successive opening and closure of three major intervening Tethyan oceans, the Paleo-Tethys (Devonian-Triassic), Meso-Tethys (late Early Permian-Late Cretaceous), and Neo-Tethys (Late Triassic-Late Cretaceous) (e.g., Metcalfe, 2013). Below we briefly introduce the geological backgrounds of the South China, Indochina, Sibumasu, and West Burma blocks, which are relevant to the discussion of the paleomagnetic data in this study.

2.1.1. South China Block

The South China Block is separated from the North China Block to the north by the Qinling-Dabie-Sulu suture, from the Tibetan blocks by the Longmen Shan fold-thrust belt to the west, and by the Jingsha Jiang-Song Ma suture from the Indochina Block in the southwest (Fig. 1). The block consists of the Yangtze Craton in the northwest and the Cathaysia Fold Belt in the southeast that have been accreted to each other in the Proterozoic around 860 Ma (Li et al., 2009; Charvet, 2013; Yao et al., 2013). The South China Block collided with the North China Block between Permian (McElhinny et al., 1981; Enkin et al., 1992; Yang and Besse, 2001c) and Late Triassic time (Zhao and Coe, 1987; Gilder and Courtillot, 1997; Meng and Zhang, 1999; Huang et al., 2008). The South and North China Blocks were probably part of stable Eurasia since the latest Jurassic-earliest Cretaceous closure of the Mongol-Okhotsk ocean (Liu and Morinaga, 1999; Morinaga and Liu, 2004; Zhu et al., 2006; Tsuneki et al., 2009; Cogné et al., 2005; Van der

Voo et al., 2015). During Late Cenozoic deformation in Tibet, a part of the South China Block in the southwest became separated along the Xianshuihe-Xiaojiang left-lateral strike slip fault and is now known as the Chuandian terrane (e.g., Wang et al., 1998a; Zhu et al., 2008; Li et al., 2013a; Tong et al., 2015; Wang et al., 2016, Figs. 1 and 2). The eastern coast of the South China Block has been moderately affected by deformation associated with Pacific subduction (Li et al., 2005; Sun et al., 2006; Wang and Yang, 2007). The South China Block referred to in this study does not include the Chuandian terrane, which will be discussed separately.

2.1.2. Indochina Block

The Indochina Block is bounded by the Jingsha Jiang-Song Ma suture to the northeast, and the Changning-Menglian-Chiang Mai-Inthanon suture zone to the west (Metcalfe, 2013, Fig. 1). The Song Ma suture is generally regarded as a branch of the Paleo-Tethys, while the Changning-Menglian-Chiang Mai-Inthanon suture zone represents the main remnant of the Paleo-Tethys ocean (Wu et al., 1995; Metcalfe, 1996; Zhong, 1998). The Indochina Block, like the South China Block, is also thought to have derived from the NE of Gondwana in the Early Paleozoic, and rifted and drifted to the north since the Devonian. The timing and style of collision between Indochina and South China remain controversial, and estimated collision ages range from the Triassic, Early Paleozoic or Middle Carboniferous along the Song Ma, Song Da or Dianqiong suture zone (Cai and Zhang, 2009; Faure et al., 2014, Fig. 1). In the Cenozoic time, the Indochina Block became separated from the South China Block along the Ailao Shan-Red River fault zone, which roughly follows the Jingsha Jiang-Song Ma suture.

2.1.3. Sibumasu Block

The Sibumasu Block is inferred to be an eastern extension of the Qiangtang Block of Tibet, and is thought to have formed an eastern continuation of the Cimmerian continental fragments of Iran and Afghanistan (Şengör, 1984). It is bounded to the west and southwest by the Mogok Metamorphic Belt, the Andaman Sea, and the Medial Sumatra Tectonic Zone (Barber and Crow, 2009). To the east the Changning-Menglian-Chiang Mai-Inthanon and Bentong-Raub suture zones separate Sibumasu from the Indochina and East Malaya further to the east (Fig. 1). The Sibumasu/Qiangtang Block is thought to have rifted from Gondwana in the Early Permian (Fang et al., 1989; Huang and Opdyke, 1991a; Metcalfe, 2002). It separated from Gondwana and drifted to the north, opening Meso-Tethys in its wake. The Sibumasu Block collided with Indochina in Late Triassic time, which marks the closure of Paleo-Tethys (Carter et al., 2001; Sone and Metcalfe, 2008; Jian et al., 2009; Wang et al., 2010b; Zhao et al., 2015).

2.1.4. West Burma Block

The West Burma Block is bounded by Mogok metamorphic belt-Sagaing fault to the east and the Indo-Burma Ranges to the west (Fig. 1). The tectonic affiliation of the West Burma Block is hotly debated in the past, which hinges on whether it is correlated to the Lhasa block (Mitchell, 1993; Searle et al., 2007) or to the West Sumatra block (Barber and Crow, 2009). However, based on detailed petrology, XRD diffraction, heavy mineral and detrital zircon U-Pb data, Sevastjanova et al. (2016) argued that the West Burma Block was part of Eurasia from the late Triassic. After the Late Cretaceous, it moved northwards along the Gaoligong/Sagaing fault during the India-Asia collision.

2.2. Cenozoic tectonic deformation of southeast Tibet

The southeast margin of Tibet Plateau is intensely deformed since Late Cretaceous and particularly Cenozoic time due to convergence and collision between India and Eurasia. As a result, a series of regional north- and northwest-striking strike-slip faults (e.g., Wang et al., 1998a,

Table 1
A review on strike-slip faults in the southeast margin of Tibetan Plateau.

Fault name	Fault length (km)	Sense	Displacement (km)	Age (Ma)	Reference
Ailao Shan-Red River shear zone	> 900	L	700 ± 200 ~600	35–17	Leloup et al. (1995, 2001) Chung et al. (1997)
Chongshan shear zone	250	L	Unknown	32–21 32–27 32–22	Hall (2002), Searle et al. (2010), Mazur et al. (2012) Wang et al. (2006) Zhang et al. (2010)
Gaoligong shear zone	600	L + R R	Unknown	34–17 18–13 32–17	Akciz et al. (2008) Lin et al. (2009), Zhang et al. (2012a) Wang et al. (2006), Akciz et al. (2008)
Wangchao/Maoping shear zone	450	L	150–160	40–30	Tapponnier et al. (1982), Lacassin et al. (1997), Morley (2007)
Three Pagodas shear zone	250	L	160	36–33	Lacassin et al. (1997)
Sagaing fault		R	460	11	Mitchell (1993), Curray (2005), van Hinsbergen et al. (2011a)
Xianshuihe-Xiaojiang fault		L + N	78–100	13	Roger et al. (1995), Zhang et al. (2004), Wang et al. (2009), Li et al. (2015)
Red River fault		R	40	8	Allen et al. (1984), Wang et al. (1998a), Replumaz and Tapponnier (2003), Schoenbohm et al. (2006a), Li et al. (2013a)
Dayingjiang	135	L + N	4	Unknown	
Ruili fault		L + N	11	Unknown	Wang et al. (2014)
Wanding fault	170	L	10	Pliocene?	Lacassin et al. (1998), Wang and Burchfiel (1997)
Nanting river fault	380	L	8	5	Lacassin et al. (1998)
			40–50	Pre-Pliocene	Wang and Burchfiel (1997)
			21		Wang et al. (2014)
Lingcang/Heihe fault	210	L	30	Pliocene?	Wang and Burchfiel (1997)
		R	17	5	Wang et al. (2014)
Dien Bien Phu fault	150	L	12.5	5	Lai et al. (2012)
			Unknown	130, 29–26	Bui et al. (2017)
Mengxing fault	180	L	24	Unknown	Lacassin et al. (1998), Wang et al. (2014)
Wan Ha fault	140	L	6	Unknown	Wang et al. (2014)
Jinghong fault	110	L	11	Unknown	Wang et al. (2014)
Menglian fault	120	L	5.5	Unknown	Wang et al. (2014)
Lashio fault	85	L	2.5–6.5	Unknown	Wang et al. (2014)
Kyaukme fault	210	L	2.6	Unknown	Wang et al. (2014)
Nam Ma fault	215	L	13	Unknown	Wang et al. (2014)
Mae Chan fault	310	L	4	Unknown	Wang et al. (2014)

L: left-lateral, R: right-lateral, N: normal.

Fig. 2), tight folds with NW-NNW-trending axes in Mesozoic-Cenozoic red beds, and a physiography of high elevation mountainous regions with low-gradient plateau margin and low-relief relicts that are deeply incised by continental scale rivers (Clark et al., 2006; Liu-Zeng et al., 2008) were formed during the Cenozoic.

Owing to variation in the amount of Cenozoic exhumation, the major strike-slip systems in and around the Indochina and Sibumasu blocks are exposed as ductile, metamorphic shear zones, such as the Ailao Shan, Chongshan, Gaoligong, and Mogok shear zones, or brittle faults, such as the Xianshuihe-Xiaojiang, Red River, and Sagaing faults (Fig. 2, Table 1).

The left-lateral Xianshuihe-Xiaojiang fault is one of the most important faults in SE margin of the Tibetan Plateau that accommodate diffuse deformation and differential rotations around the eastern Himalayan syntaxis (Schoenbohm et al., 2006a; Wang et al., 1998a). It has a length of > 1000 km, extending from eastern Tibet in the northwest to the south of Yunnan and terminating before reaching the Red River fault (Fig. 2). The total offset along the Xianshuihe-Xiaojiang fault, which is about 80–100 km, is partitioned along the numerous branching faults or transferred to extension locally, resulting in a number of basins (Wang et al., 1998a, 2008b). The Xianshuihe-Xiaojiang fault initiated at ~13 Ma (Roger et al., 1995; Zhang et al., 2004; Wang et al., 2009; Li et al., 2015), but some fault branches may have begun as late as ~5 Ma (Zhu et al., 2008; Wang et al., 2009), separating the Chuandian terrane from the South China Block.

The left-lateral Ailao Shan-Red River shear zone lies at the basis of the Indochina extrusion model (Tapponnier et al., 1982, 1990; Leloup et al., 1995). It is associated with four metamorphic complexes: the Xuelong Shan, Diancang Shan, Ailao Shan and Day Nui Con Voi complexes from SW China, through Vietnam, and towards the South China Sea along the southwestern margin of the South China Block

(Leloup et al., 1995, Fig. 2). The well-developed foliation and lineation in the metamorphic rocks indicate sinistral shearing during the ductile deformation. Controversy exists on the timing and amount of displacement of the Ailao Shan-Red River shear zone. One school of thought argues that the sinistral slip along the lithosphere-scale Ailao Shan-Red River shear zone occurred between 34 and 17 Ma (Schärer et al., 1990, 1994; Leloup et al., 1995, 2001; Zhang and Schärer, 1999; Gilley, 2003). Using geological markers such as ophiolite belts, Mesozoic red bed basins, Upper Permian basalts, Triassic arc volcanics, and belts of Cretaceous granites and norites exposed on either side of the north-western part of the Ailao Shan-Red River shear zone, estimates of sinistral displacement were made of 700 ± 200 km (Leloup et al., 1995; Chung et al., 1997), or even as large as 1500 km (Yang and Besse, 1993). The displacement of the Ailao Shan-Red River shear zone in this school of thought was kinematically linked to and accommodated by the opening of the South China Sea (Briaies et al., 1993). Another school of thought, however, based estimates on the amount of displacement on structural offshore northern Vietnam as well as kinematic reconstructions of SE Asia, argued for displacement of no more than some 250 km at the southern end of the fault (Wang and Burchfiel, 1997; Hall, 2002; Searle, 2006; Searle et al., 2010; Clift et al., 2008; van Hinsbergen et al., 2011a; Mazur et al., 2012), with an age of slip ranging from 32 to 22 Ma (Searle et al., 2010; Cao et al., 2011; Liu et al., 2012), or as short as 27–22 Ma (Wang et al., 1998b). How these estimates should be reconciled remains enigmatic and will be discussed in this paper. In its latest motions, since the Late Miocene, Red River fault inverted (Leloup et al., 1993; Schoenbohm et al., 2006b; Li et al., 2013a) and accommodated ~40 km right-lateral strike-slip displacement (Allen et al., 1984; Wang et al., 1998a; Replumaz and Tapponnier, 2003; Schoenbohm et al., 2006b).

To the west of Sibumasu, the N-S striking Sagaing fault is a 1200 km

long, currently active, right-lateral strike-slip fault that has accommodated Late Cenozoic northward motion of the West Burma Block relative to Sibumasu (Fig. 2). This northward motion is interpreted as the result of strain partitioning of the highly oblique convergence between India and Sibumasu, whereby the Sagaing fault accommodates the northward component of motion, and the eastward component of motion is taken up by eastward subduction below the West Burma Block (Bertrand et al., 1999; Vigny et al., 2003). It runs along most of the N-S length of Myanmar, cuts the western margin of the Mogok belt, and connects south to the active forearc spreading center in the Andaman Sea via a series of short transfer faults (Vigny et al., 2003; Curray, 2005, Figs. 1 and 2). The total displacement of the Sagaing fault is estimated about 460 km since ~11 Ma (Mitchell, 1993; Curray, 2005). To the east of the Sagaing fault lies the ductile right-lateral Gaoligong shear zone and the Shan Scarp that are regarded as the western boundary of the extruding Indochina-Sibumasu domain during the Cenozoic prior to the activity of the Sagaing fault (Bertrand et al., 1999, 2001; Socquet and Pubellier, 2005; Wang et al., 2006; Akciz et al., 2008; van Hinsbergen et al., 2011a). Geochronological data suggested that the strike-slip shearing along the Gaoligong shear zone and Shan Scarp occurred between the Oligocene and Middle Miocene (Bertrand et al., 2001; Wang et al., 2006; Searle et al., 2010; Zhang et al., 2012a), contemporaneous with the left-lateral strike-slip on the Ailao Shan-Red River shear zone. There is no field-based estimate on the total amount of dextral strike-slip along the Gaoligong shear zone and Shan Scarp, although van Hinsbergen et al. (2011a) tentatively suggested some 500–600 km to restore the West-Burma Block south of the Late Eocene-Oligocene Wang Chao and Three Pagodas faults that have no continuation in the West Burma Block.

The Chongshan shear zone is interpreted to be a conjugate shear zone to the Ailao Shan-Red River and Gaoligong shear zones to accommodate the southeastward extrusion of Indochina/Sibumasu (Socquet and Pubellier, 2005; Wang et al., 2006; Akciz et al., 2008; Zhang et al., 2010, Fig. 2). Structural studies suggested that the shear zone comprises both dextral and sinistral strike-slip shear from Oligocene to Middle Miocene times (Akciz et al., 2008; Zhang et al., 2010). Thus, the region between the Gaoligong Shan shear zone and the Ailao Shan-Red River shear zone was cut into two segments by the Chong Shan shear zone (Akciz et al., 2008; Zhang et al., 2010).

The left-lateral Wang Chao (also named Mae Ping) and Three Pagodas shear zones were regarded as boundaries of the earliest stage of Indochina's extrusion during Late Eocene-Early Oligocene time (Lacassin et al., 1997; Morley, 2007, Fig. 2). The offset along the Wangchao and Three Pagodas shear zone is estimated at about 160 km each (Lacassin et al., 1997; Morley, 2007).

Except the large-scale Sagaing, Xianshuihe-Xiaojiang and Red River fault, which are hundreds to more than a thousand kilometers long, numerous smaller strike-slip faults (roughly 100 to about 200 km long) developed in the SE margin of the Tibetan Plateau, especially the region southwest of the Red River fault (Fig. 2). These faults include a set of NE-SW, left-lateral faults and one NW-SE, right-lateral fault. The most prominent of these are Ruili, Wanding, Nanting, Mengxing, Mae Chan, and Dien Bien Phu faults (Fig. 2). Based on geomorphology, river bends across the faults, and fault bounded basins, most of these faults are suggested to be left-lateral, active at least in Late Miocene or Pliocene times but possibly before, with at least tens of kilometers displacement (Wang and Burchfiel, 1997; Wang et al., 1998a; Lacassin et al., 1998; Socquet and Pubellier, 2005; Wang et al., 2008a, 2014, see Table 1 for details). Some of the rivers show hairpin geometries when crossing these active strike-slip faults, which may suggest a regional reversal of slip sense from right to left-lateral sometime between 5 and 20 Ma (Lacassin et al., 1998). However, the detailed slip history of these faults remains poorly constrained.

3. Paleomagnetic data compilation

3.1. Data selection

We compiled a comprehensive paleomagnetic dataset based on 177 paleomagnetic sites based on 17,179 paleomagnetic directions from 81 paleomagnetic studies from Jurassic and younger rocks from South China, Indochina, and the Sibumasu Block. Paleomagnetic data were not included if they: (1) came from rocks older than Triassic or Quaternary and younger; (2) came from studies that do not provide information on demagnetization procedures; (3) were not analyzed by principle component analysis; (4) were (likely) remagnetized according to the original authors; and (5) if site *k*- or *K*-values (precision parameters of Fisher (1953) on directions or poles, respectively) are lower than 7 for sediment sites and 50 for volcanics. Since many of the available paleomagnetic data are derived from Cretaceous rocks deposited during the Cretaceous normal superchron, the presence of reversals is not a general requirement. Remagnetized directions with precise age constraints on magnetization acquisition (e.g., Kornfeld et al., 2014c; Li et al., 2017), and anomalous directions due to local tectonics as pointed out by the original authors (e.g., Tong et al., 2013), are presented but not included in the final discussion.

3.2. Paleomagnetic data compilation

Paleomagnetic data are typically provided in the literature as site averages of paleomagnetic directions and described using Fisher (1953) statistics. Subsequently, such site averages are then averaged to obtain a regionally meaningful paleomagnetic direction. Such an approach gives equal statistical weight to every site average, even though the number of data per site may strongly vary. The main source of scatter in paleomagnetic data derives from paleosecular variation (PSV) of the geomagnetic field, which provides an angular dispersion of tens of degrees (e.g., Butler, 1992; Tauxe and Kent, 2004; Johnson et al., 2008; Deenen et al., 2011). On time scales of tens to hundreds of thousands of years, paleosecular variation averages out, and therefore, paleomagnetists collect a large number of specimens from sedimentary rocks, or a large number of lava sites, to approximate the paleomagnetic pole. Given the large dispersion of paleomagnetic directions due to PSV, large sites will provide a more reliable paleomagnetic direction than small sites, and we therefore aim to weigh the statistical importance of sites as a function of the amount of samples that they were based on (see Deenen et al., 2011). To that end, we aim to combine all paleomagnetic directions (*n*) of a set of sites from a region rather than site averages to come to an average paleomagnetic pole. As a test to identify whether major internal vertical axis rotations occurred in a region, we test whether the obtained paleomagnetic scatter, expressed as the A95 around the paleomagnetic pole, can be straightforwardly ascribed to PSV, following the *n*-dependent reliability criteria of Deenen et al. (2011). Unfortunately, the original individual specimen directions are seldom provided in the published literature. We therefore parametrically sampled *n* directions from a site that was based on *n* specimens, randomly drawing these from a distribution with a Fisher (1953) precision parameter *K* (on virtual geomagnetic poles (VGPs) as reported from that site, using the online paleomagnetic analysis tool www.paleomagnetism.org (Koymans et al., 2016)). Most paleomagnetic studies do not provide the *K* values, but instead report the *k* parameter, which is the precision parameter on paleomagnetic directions instead of VGPs. The *k* value is generally somewhat higher than the *K* value. An estimate of *K* can be made from *k* if the paleolatitude of the site is known (e.g., Deenen et al., 2011), but since most sites come from clastic sediments prone to inclination shallowing, this correction introduces another uncertainty. We have therefore taken a simplified approach and assumed *k* and *K* are equal – which leads to similar results when tested against real data from Indochina of Li et al. (2017). This means in practice that the data scatter that results from our parametric sampling

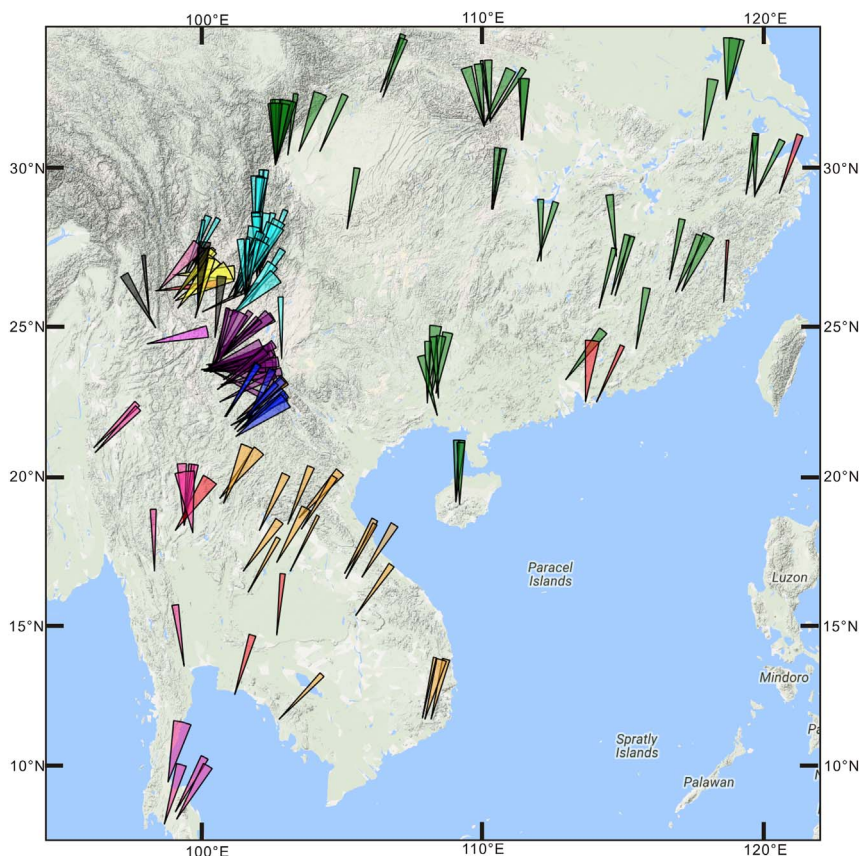


Fig. 3. Map with locations and declinations of the paleomagnetic sites marked with different colors from South China Block and southeast margin of the Tibetan Plateau. The green and cyan represent the rigid South China Block and Chuandian terrane, respectively. The orange, blue, purple, and yellow represent the four sub-terrane of Southern Indochina, Southern Simao, Northern Simao, and Lanping, respectively (see detailed explanation in text). The pink represents data from the Sibumasu Block. The red represents paleomagnetic data from rare volcanic or plutonic sites, while the black represents outlying directions that reflect localized deformation. (For interpretation of the references to colour in this figure legend, the reader is referred to the web version of this article.)

approach may somewhat overestimated and provides a conservative estimate of the real scatters involved in the original data. All the reversed polarity directions are flipped to the normal polarity directions. The site averages in our compilation are based on the parametrically sampled sites, and may thus deviate slightly from the published averages. All data files, and references to the published literature on which they are based, are provided in the Supplementary Information 1.

4. Results

4.1. Data integration

We compare the paleomagnetic data from our database against the Global Apparent Polar Wander Path (GAPWaP, Torsvik et al., 2012) rotated in Eurasian coordinates. We computed the declinations and inclinations at reference points 30°N, 105°E for the South China Block, and 23°N, 100.8°E for Indochina. The compiled paleomagnetic data are plotted in different tectonic blocks with different colors (Fig. 3): the Chuandian Terrane is marked in cyan to be distinguished from the rigid South China Block (marked in green). Since the paleomagnetic declinations in Indochina Block exhibit systematic variation in different parts (see detailed explanation below, Fig. 4), we choose the known faults (Dien Bien Phu, Lancang, and Nanting faults) in the interior of the Indochina Block as boundaries and separate the Indochina Block into four sub-terrane (Fig. 4): Southern Indochina (Vietnam in Royden et al., 2008, marked in orange), Southern Simao (marked in blue), Northern Simao (marked in purple), and Lanping (marked in yellow). In addition, paleomagnetic data from rare volcanic or plutonic sites are

marked in red; outlying directions that reflect localized deformation as interpreted by the original author or later studies are marked in black (Figs. 3 and 4).

The averages of each sub-terrane are calculated based on both site and individual, parametrically sampled direction averages (Figs. 5 and 6). Age estimates on sampled sedimentary sections are typically within a geologic period with age errors spanning an entire period, e.g., Early Cretaceous (145–100 Ma) was assigned at 122.5 Ma with an error of 22.5 Ma. The following ages are generally constrained: Early, Middle, and Late Jurassic, Early and Late Cretaceous, Paleocene, Eocene, Oligocene and Mio-Pliocene. We also calculate independent APWPs for the South China Block, Southern Indochina, Southern Simao and Northern Simao based on available data (Table 2), which we computed in 10 Myr time intervals from 180 to 40 Ma, using a 20 Myr sliding window, which is the same approach as used in the reference GAPWaP (Torsvik et al., 2012). We computed the APWP using site averages (i.e., the approach used in calculating the GAPWaP that does not take within-site uncertainties into account), and on individual direction averages that does take the data amount and dispersion of each site into account.

4.2. Inclination trends

Inclinations of sites or combined poles of all blocks are consistently lower than those predicted by the Eurasia APWP (Figs. 5–7). The newly calculated South China APWP provides an inclination that is consistently $\sim 20 \pm 5^\circ$ shallower than predicted by the Eurasian APWP for the Cretaceous and Paleogene (Fig. 7). The few data points from volcanic rocks of the Cretaceous of the South China Block (red dots in Fig. 5) are close to or within error of the predicted paleolatitude

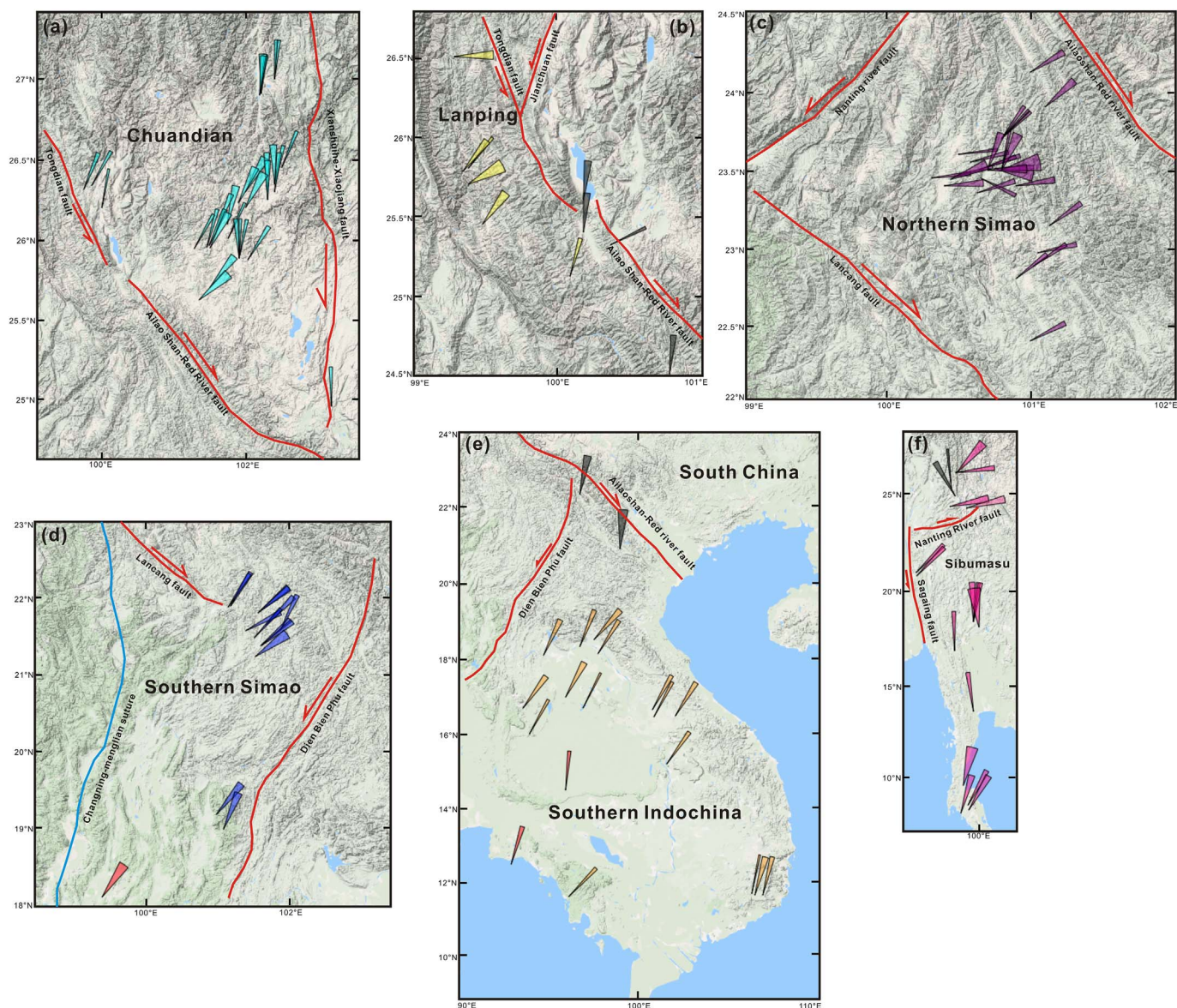


Fig. 4. Enlarged map showing the boundaries and variations of paleomagnetic declinations of different blocks. Colors are the same as Fig. 3. (For interpretation of the references to colour in this figure legend, the reader is referred to the web version of this article.)

(Fig. 5). The inclinations of the Indochina Block show inclinations that are generally similar to or lower than the expected inclination for Eurasia (Figs. 5 and 6), but are somewhat steeper than those compiled from the South China Block. The few sites of Wang and Yang (2007) and Tong et al. (2013) that are corrected for inclination shallowing provide inclinations that are generally equal, or only a few degrees lower relative to Eurasia (red open circles in Figs. 5 and 6).

4.3. Vertical axis rotations

Paleomagnetic declinations from the South China Block cluster around the GAPWaP in Eurasian coordinates (Figs. 5 and 7), confirming that the South China Block did not experience a significant rotation with respect to Eurasia ($< \sim 5^\circ$) since the latest Jurassic. Some Eocene rocks of the South China Block indicate $\sim 10^\circ$ counterclockwise rotation but these sites are located close to the left-lateral Xianshuihe-Xiaojiang fault and probably recorded local strike-slip-related rotations (Fig. 3). Most declinations in the Indochina Block are positive ($\sim 10\text{--}80^\circ$, Fig. 6), and their values vary from block to block (Fig. 6), which is much clearer in the GAPWaPs (Fig. 7). The Jurassic to Cretaceous paleomagnetic

declinations exhibit uniformly a $\sim 15^\circ$ clockwise rotation for the Southern Indochina (Fig. 4e), $\sim 40^\circ$ in the Southern Simao terrane (Fig. 4d) and $\sim 60\text{--}80^\circ$ in the Northern Simao terrane (Fig. 4c), and $\sim 40^\circ$ in the Lanping terrane in the northwest (Fig. 4b). An important implication of this pattern is that deformation of the Indochina and Sibumasu blocks in the region of the southeast margin of the Tibetan Plateau can be approximated by quasi-rigid rotating blocks separated by (transpressive) strike-slip faults. The Cenozoic paleomagnetic data from the Northern Simao terrane suggest a rapid rotation between Eocene and Middle Miocene (Figs. 6 and 7). The paleomagnetic declinations of Chuandian terrane show systematic decrease from $\sim 40^\circ$ to 0° from southwest to the northeast close to the Xianshuihe-Xiaojiang fault (Fig. 4a). The paleomagnetic declinations in the Sibumasu Block change gradually from clockwise rotation ($\sim 90^\circ$) in the north of Tengchong area to counterclockwise rotation in the south-central, and to clockwise rotation (20°) again in the southern part (Fig. 4f). The variation trend generally mimics the sinusoidal shaped mountain belt in the western margin of Sibumasu Block, suggesting that the west boundary of the Sibumasu Block was originally a straight structure, but evolved into a sinusoidal-shaped structure in the Cen-

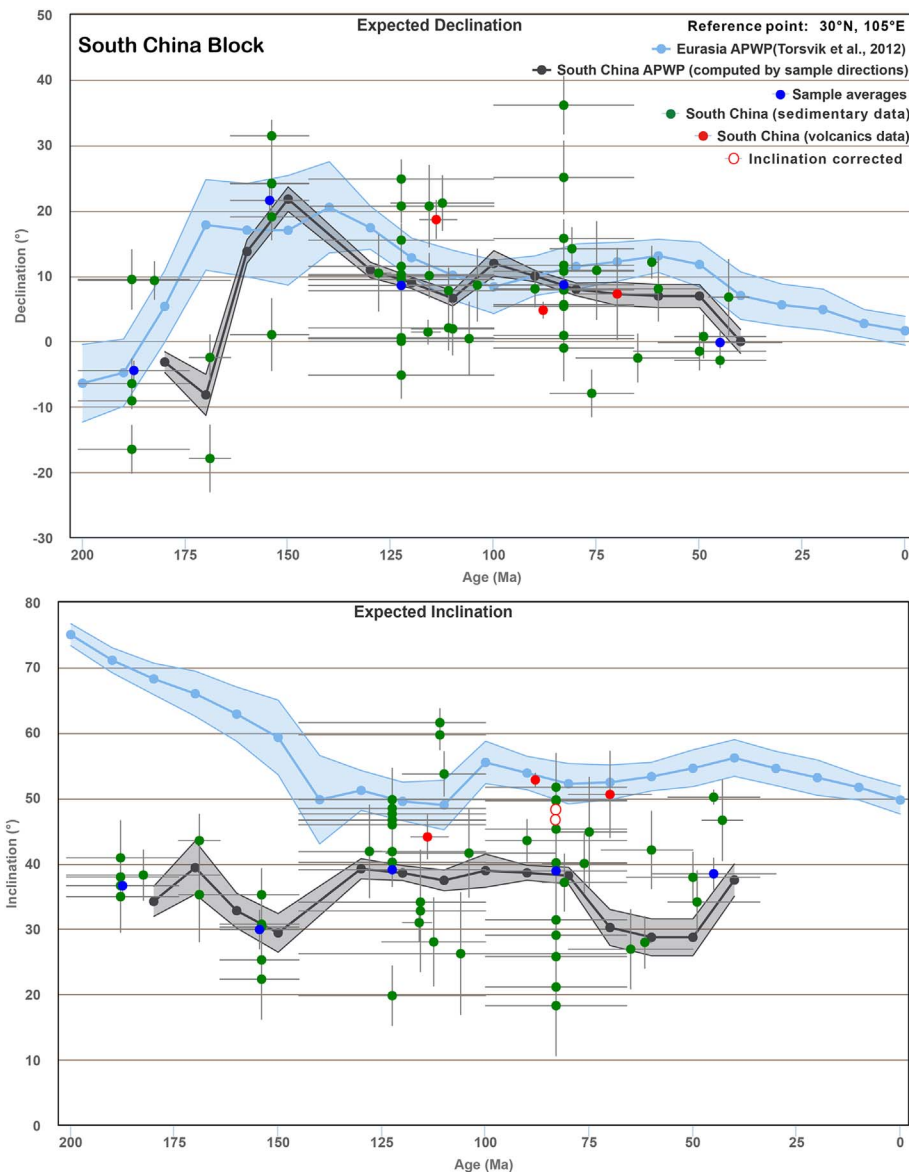


Fig. 5. The compiled paleomagnetic directions (declinations and inclinations, marked in green for sedimentary data and red for volcanic data), sample averages (in blue), and the computed apparent polar wander path (APWP) by using individual direction averages (in black with light grey envelope of errors) from the South China Block versus age at a reference point of 30°N, 105°E and their comparison with the expected directions from the APWP of Eurasia (Torsvik et al., 2012, marked in blue circles with light blue envelope of errors). (For interpretation of the references to colour in this figure legend, the reader is referred to the web version of this article.)

ozoic due to internal rotational deformation (Wang and Burchfiel, 1997; Yamashita et al., 2011). Only small declinations ($\sim 0\text{--}10^\circ$) are present along the Ailao Shan-Red River fault suggesting only minor drag folding may have occurred here (Fig. 4b and e). Other clusters of small to negative declinations can be observed along the Xianshuihe-Xiaojiang fault in the Chuandian Terrane and along Gaoligong fault in the Sibumasu Block (Fig. 4a and f).

5. Discussion

5.1. Inclination shallowing and paleolatitude interpretation

An important observation of the compiled paleomagnetic data is that paleomagnetism provides no solid basis to infer significant, paleomagnetically resolvable southward motion of the Indochina Block with respect to Eurasia. In fact, when inclinations are straightforwardly translated into paleolatitudes, the paleomagnetic data from the South China Block would even suggest a > 2000 km northward motion with respect to Eurasia, which is in stark contrast to geological

evidence. However, because most of the paleomagnetic studies were undertaken on clastic sedimentary rocks, which are notoriously vulnerable to compaction-induced inclination shallowing (e.g., Kodama and Sun, 1992; Kodama, 2012; Gilder et al., 2001; Tan et al., 2003; Tauxe and Kent, 2004; Yan et al., 2005; Huang et al., 2013; Li et al., 2013a, b), this apparent northward motion is probably an artifact of such compaction. This conclusion is in line with the few inclinations derived from volcanics-based data from the South China Block that are in good agreement with the expected inclination from Eurasia (Chan, 1991; Wang et al., 2010a; Huang et al., 2012, Fig. 5).

In addition, a few studies applied the E/I method of Tauxe and Kent (2004) to correct the bias of inclination shallowing (Wang and Yang, 2007; Tong et al., 2013, 2015). We also conducted E/I corrections for studies that we have the original data (Zhu et al., 2008; Li et al., 2013a, 2015, 2017). As shown in Table 3, except the results of Tong et al. (2015), which still show a much shallower inclination after correction with respect to Eurasia, the other corrected inclinations are roughly consistent with the Eurasian reference frame (Figs. 5 and 6). These results suggest that the lower than expected inclinations for the

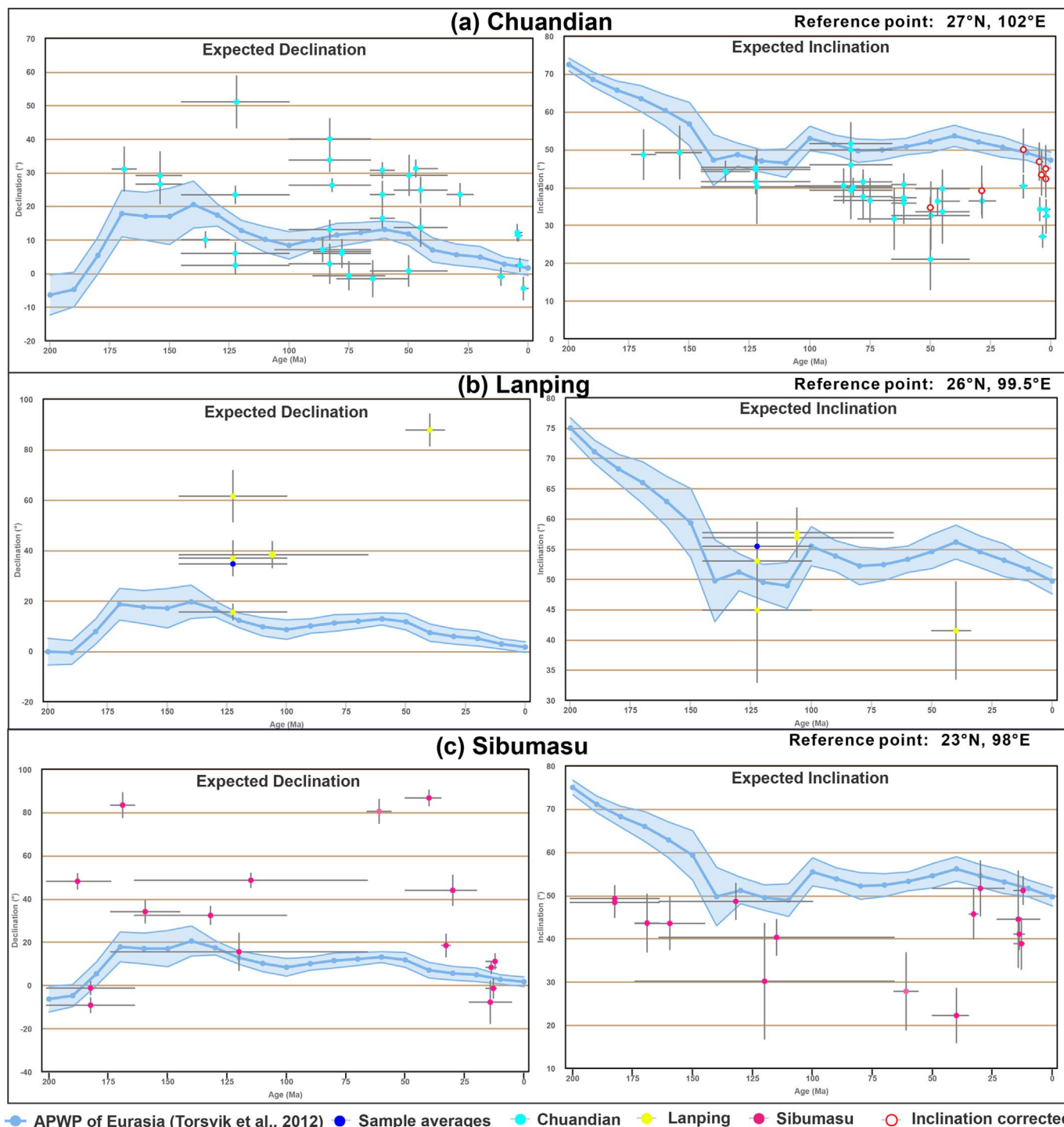


Fig. 6. The compiled paleomagnetic directions (declinations and inclinations), sample averages (in blue), and the computed apparent polar wander path (APWP) by using individual direction averages (in black with light grey envelope of errors) from (a) Chuandian terrane, (b) Lanping, (c) Sibumasu, (d) Northern Simao, (e) Southern Simao, and (f) Southern Indochina Blocks versus age and their comparison with the expected directions from the APWP of Eurasia (Torsvik et al., 2012, marked in blue circles with light blue envelope of errors). (For interpretation of the references to colour in this figure legend, the reader is referred to the web version of this article.)

sedimentary rocks is most likely due to compaction-induced inclination shallowing. However, the inferred flattening factors from these studies differ (ranging from 0.4 to 0.8, Table 3), and therefore cannot be used as a firm reference to correct other sites. Paleomagnetic data from the Indochina and Chuandian blocks give somewhat steeper inclinations than those for the South China Block (Fig. 7), which allows for some southward motion of these blocks relative to the South China Block (this is actually most of previous paleomagnetic studies adopted) if compaction is everywhere equal, as required by the motion along the

Xianshuihe-Xiaojiang and Ailao Shan-Red River faults, but paleomagnetic data, particularly with the uncertainties in amount of inclination shallowing, cannot quantify this motion, which should therefore rely on structural geological arguments. We note that even the largest estimates of displacement along the NW-SE striking Ailao Shan-Red River fault would produce only a few degrees of southward motion relative to the South China Block, which is unresolvable, but permitted by paleomagnetic constraints.

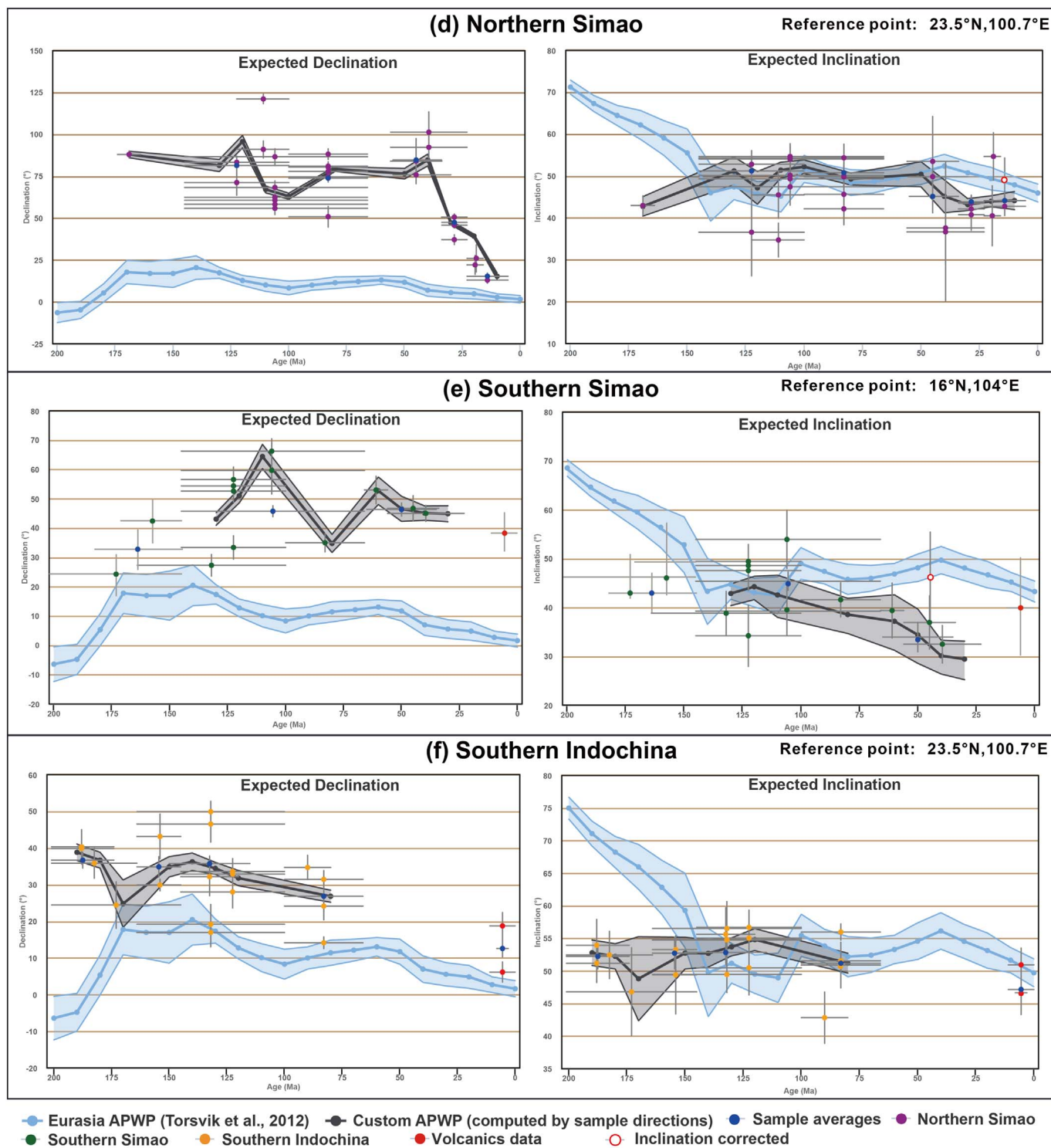


Fig. 6. (continued)

5.2. New reconstructions of Cenozoic deformation of Indochina

5.2.1. A new tool to test kinematic restorations against paleomagnetic data

Paleomagnetic data record motion of geological units relative to the geodynamo, which on geological timescales can be assumed to coincide with the Earth's spin axis (e.g., [Butler, 1992](#)). Paleomagnetic data can be used to quantitatively inform kinematic reconstructions, which describe relative motions between geological units on a sphere using Euler's theorem. There are, however, an infinite number of Euler rotations that correctly describe paleomagnetic data, and additional

structural geological constraints are required to develop kinematic restorations.

We therefore designed an additional tool on the recent open-access, online platform for paleomagnetic analysis [Paleomagnetism.org](#) ([Koymans et al., 2016](#)) that allows testing of kinematic restorations against paleomagnetic data (see tutorial in the Supplementary Information 2). This tool allows to rotate the GAPWaP (whereby we use [Torsvik et al. \(2012\)](#)'s version) into the coordinates of a reconstructed block if the Euler poles of this block are provided in 10 Myr intervals relative to South Africa.

Table 2
Mean paleomagnetic poles of South China, Southern Indochina, Southern Simao and Northern Simao blocks computed on available data by average sites and average individual sample directions.

South China APWP-averaging sites				Southern Indochina APWP-averaging sites				Northern Simao APWP-averaging sites				Southern Simao APWP-averaging sites							
Age (Ma)	n	Plat (°)	Plong (°)	A95 (°)	Age (Ma)	n	Plat (°)	Plong (°)	A95 (°)	Age (Ma)	n	Plat (°)	Plong (°)	A95 (°)	Age (Ma)	n	Plat (°)	Plong (°)	A95 (°)
40	4	84.4	278.0	7.8	90	4	65.1	171.8	10.4	10	3	72.7	194.8	16.4	40	2	47.8	197.1	8.2
50	5	84.1	265.0	6.3	120	3	60.5	166.9	6.1	20	6	61.2	192.8	12.1	110	2	36.5	177.7	31.7
60	5	79.9	260.1	8.8	130	8	59.3	166.4	6.8	30	5	32.7	182.6	26.6	120	4	47.5	183.8	12.3
70	6	81.1	257.3	8.3	140	5	58.6	166.1	12.1	40	4	13.6	171.6	14.2	130	5	51.4	186.8	12.4
80	16	78.5	232.2	5.7	150	2	56.6	173.3	25.9	50	2	23.9	169.1	18.9					
90	14	76.2	228.8	6.2	180	4	58.3	173.3	7.9	80	6	26.1	173.7	9.9					
100	5	79.9	232.4	10.9	190	3	54.9	172.0	3.7	100	6	35.1	174.1	8.3					
110	10	79.4	227.9	7.9						110	8	25.8	171.7	14.3					
120	18	79.2	218.7	5.0						120	4	11.2	171.5	23.9					
130	10	79.5	219.8	6.2						130	2	23.8	177.1	37.6					
150	5	66.7	228.8	10.8															
160	7	73.6	240.0	13.4															
170	2	77.9	339.3	34.3															
180	5	81.1	302.3	10.4															

South China APWP-averaging samples				Southern Indochina APWP-averaging samples				Northern Simao APWP-averaging samples				Southern Simao APWP-averaging samples							
Age (Ma)	n	Plat (°)	Plong (°)	A95 (°)	Age (Ma)	n	Plat (°)	Plong (°)	A95 (°)	Age (Ma)	n	Plat (°)	Plong (°)	A95 (°)	Age (Ma)	n	Plat (°)	Plong (°)	A95 (°)
40	306	81.0	285.1	1.7	90	592	66.9	183.5	1.4	10	342	75.8	208.2	1.7	30	194	47.9	199.8	2.6
50	453	74.0	260.1	1.7	120	243	62.8	175.3	1.7	20	1531	55.2	192.2	1.0	40	223	47.9	199.0	2.3
60	453	74.0	260.1	1.7	130	562	60.6	177.6	1.3	30	1240	48.1	189.8	1.1	50	29	47.7	194.2	4.0
70	456	74.7	257.7	1.7	140	320	59.1	179.4	2.0	40	109	17.2	173.6	3.1	60	31	43.1	188.7	4.3
80	1623	78.8	243.3	0.9	150	129	60.2	179.5	2.3	50	59	25.5	172.3	2.7	80	60	59.0	195.2	2.8
90	1724	77.8	235.3	0.8	170	36	68.5	189.4	5.6	80	666	22.9	172.3	1.3	110	89	34.5	179.2	3.6
100	393	76.6	229.1	1.8	180	225	58.7	180.2	1.8	100	474	36.9	174.5	1.5	120	418	46.2	181.6	2.1
110	1058	79.2	250.4	1.1	190	220	56.9	178.9	1.9	110	392	33.4	174.3	1.7	130	535	52.7	185.8	1.9
120	1882	78.5	238.8	0.8						120	126	9.3	167.5	3.3					
130	952	77.5	231.1	1.1						130	71	21.9	169.8	3.1					
150	409	65.5	225.8	1.8						170	51	13.7	174.0	1.8					
160	572	72.6	236.1	1.7															
170	177	79.4	330.5	2.9															

Note: The apparent polar wander paths were calculated by a moving average at 10 m.y. intervals with a sliding window of 20 m.y. n: number of sites or individual directions used to calculate the mean; Plat/Plong: latitude/longitude of the mean paleopole. A95 is the radius of a cone around a mean that contains the true mean direction with 95% probability. Reference point: 30.66°N, 104.06°E for South China Block, 23.5°N, 100.7°E for Southern Simao and Northern Simao, and 16°N, 104°E for Southern Indochina.

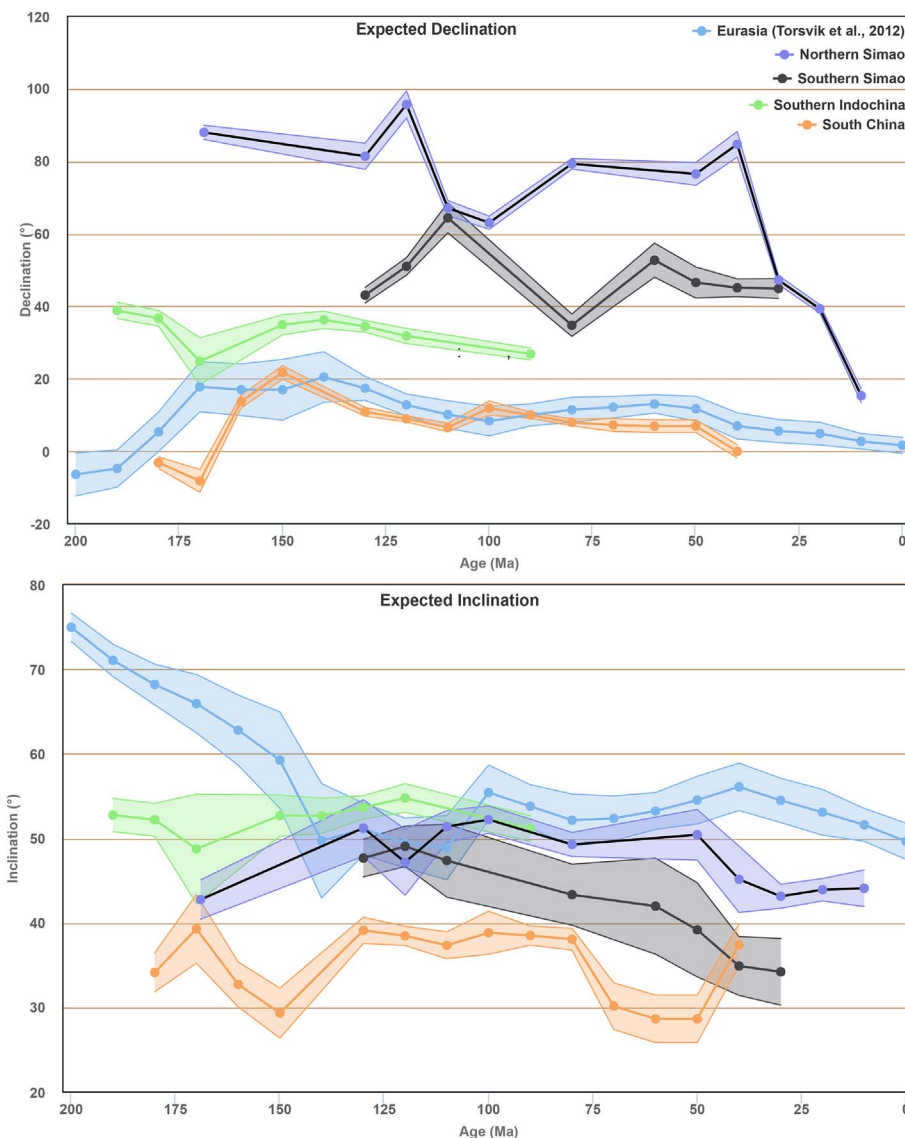


Fig. 7. A comparison of the computed APWPs of each sub-terrane using individual direction averages and the APWP of Eurasia (Torsvik et al., 2012). The declinations clearly show differential block rotations for each sub-terrane with respect to Eurasia, while the inclinations are consistently lower than those of Eurasia.

We have used this tool to test existing reconstructions of Indochina extrusion, and to develop an updated kinematic restoration of rotation and extrusion of Indochina. To this end, we reconstruct the blocks we identified based on differential rotations (Fig. 8) first relative to the

South China Block, using GPlates free plate reconstruction software (Gplates.org, Boyden et al., 2011). Small-scale motions of South China relative to Eurasia for the Neogene are reconstructed following Replumaz and Tapponnier (2003) and van Hinsbergen et al. (2011a).

Table 3
Summary of the paleomagnetic data and their E/I correction results.

Locality	Lat	Long	Age	Dec	Inc	a95	n	Inc(exp) ± ΔI	Inc(E/I)	95% range	f	Reference
Jishui [#]	27.1	115.1	K2	355.7	34.8	6.3	90	50.9 ± 3.4	48.2	40–57	0.6	Wang and Yang (2007)
Ganzhou [#]	25.9	114.9	K2	15.6	35.6	5.5	114	49.6 ± 3.4	44.4	38–52	0.7	Wang and Yang (2007)
Mengla [#]	21.5	101.5	Eocene	43.1	23.6	5.1	215	44.5 ± 3.1	44.1	38.3–49.3	0.4	Tong et al. (2013)
Jianchuan [#]	26.5	99.4	Oligocene	20.9	31.3	7.7	70	50.3 ± 3	33.9	28.3–43.2	0.8	Tong et al. (2015)
Jianchuan [#]	26.5	99.7	Eocene	29.7	32	5.6	152	49.8 ± 3.3	37.9	31.2–44.9	0.7	Tong et al. (2015)
Jinggu [*]	23.5	100.7	Miocene	13.4	30.5	3.3	108	45.4 ± 2.9	46	39.2–58.4	0.6	Li et al. (2017)
Xiaolongtan [*]	23.8	103.2	10–13 Ma	359	38.7	2.3	204	44.3 ± 2	49.5	41.6–57.7	0.7	Li et al. (2015)
Dali [*]	26.3	100	1.8–7.6 Ma	10	28.7	1.6	669	47.2 ± 2	44	40.5–47.5	0.6	Li et al. (2013a, b)
Yuanmou [*]	25.7	101.9	4.3–4.9 Ma	11.5	31.6	2.5	212	46.6 ± 2	47.7	40.5–54.1	0.6	Zhu et al. (2008)
Yuanmou [*]	25.7	101.9	2.6–4.3	1.3	26.2	2.3	219	46.6 ± 2	42.6	37.1–47.5	0.5	Zhu et al. (2008)
Yuanmou [*]	25.7	101.9	1.4–2.6	−5	25.6	1.8	515	46.6 ± 2	44.6	41.1–48.2	0.4	Zhu et al. (2008)

Lat/Long: latitude/longitude of the sample locality; K2: late Cretaceous; Dec/Inc/a95: declination/inclination and the 95% cone of confidence (reported by original authors); n: number of samples that used for E/I correction; Inc(exp) ± ΔI: the expected inclination from the Eurasia pole (Torsvik et al., 2012) and attendant confidence limits; Inc(E/I): the inclination after E/I correction; f: flattening factor; # and * represent the E/I results from literature and newly calculated in this study, respectively.

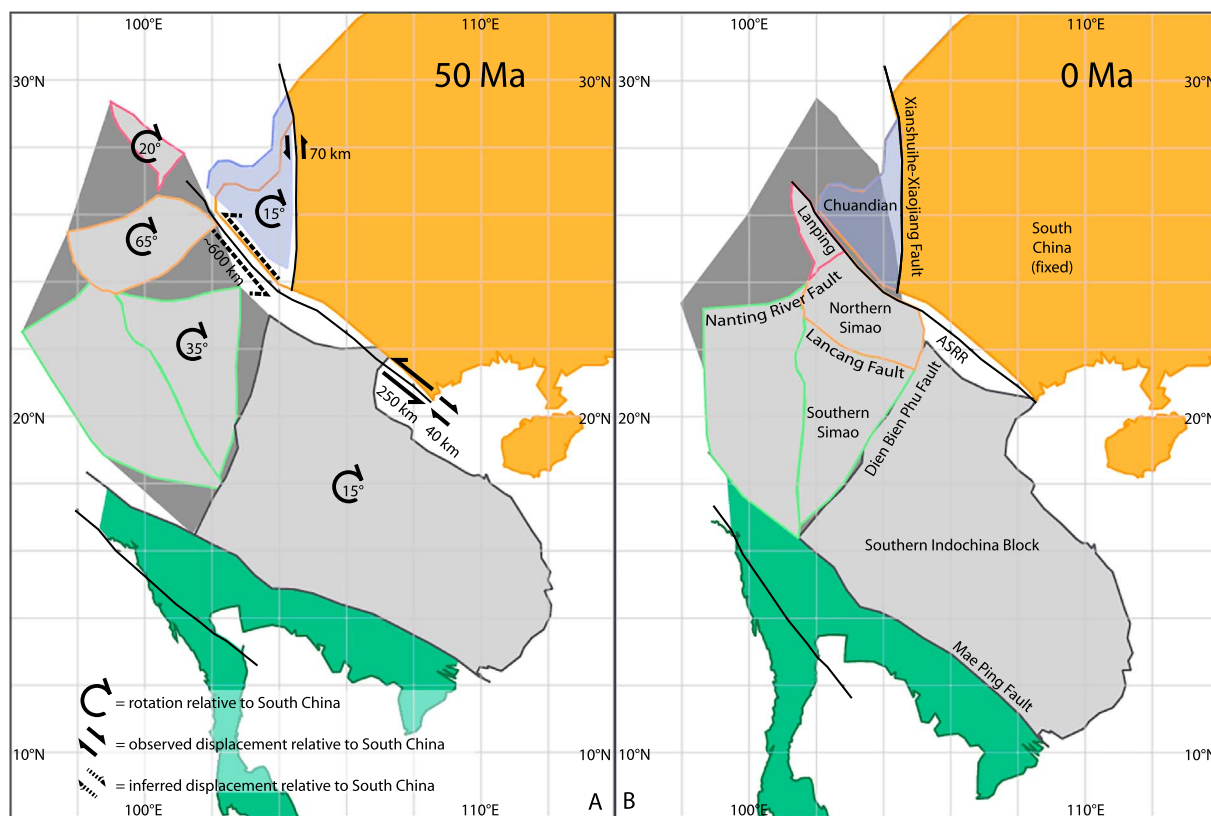


Fig. 8. Reconstruction of southeast margin of the Tibetan Plateau in a South China-fixed reference frame at (a) 50 Ma and (b) 0 Ma. The inferred rotation and displacement along the Ailao Shan-Red River fault (ASRR) are marked in Fig. 8a. The grey areas denote the shortening during the Cenozoic extrusion and rotation of Indochina.

Eurasia is reconstructed relative to South Africa using Euler rotations as detailed in Seton et al. (2012), updated with Neogene North Atlantic reconstructions of DeMets et al. (2015). The NW Indochina reconstruction is informed by structural constraints, and assumptions, as detailed below, and rotations were iteratively improved to become consistent with the paleomagnetic data reviewed above within those structural constraints.

5.2.2. Paleomagnetic tests of existing reconstructions

In the past few decades, contrasting reconstructions were proposed based on selected paleomagnetic as well as structural geological data. We will briefly show how these reconstructions compare with the paleomagnetic data compiled in our study of stable, Southern Indochina, after which we propose an improved restoration that attempts to reconcile structural and paleomagnetic data.

Lee and Lawver (1995) inferred ~500 km sinistral motion on the Ailao Shan-Red River (Fig. 9a) between 44 and 20 Ma, based on estimates by Wu et al. (1989) and Tapponnier et al. (1990) on the Ailao Shan metamorphic belt. They inferred that from 15 Ma onward the Ailao Shan-Red River fault accommodated a minor dextral displacement, based on inverted structures in the Pearl River Mouth Basin and the Beibu Gulf (Wang et al., 1989). Because they treated Indochina along the entire length of the Ailao Shan-Red River fault as a rigid block – an assumption made in most reconstructions, the predicted displacement along the southeastern end of the Red River fault is considerably larger than the estimated 250 km (Wang and Burchfiel, 1997; Fyhn et al., 2009), but the latter estimates were not yet available when Lee and Lawver published their model. The model predicted ~18° clockwise rotation of Indochina relative to South China from 44 Ma to present day, reasonably consistent with the ~15° clockwise rotation of Southern Indochina observed from paleomagnetic data, as also seen in the predicted declinations using the Euler rotations that we estimated from their reconstruction computed relative to Africa (Fig. 10a).

Hall (2002) loosely inferred that Indochina may have undergone net NW-SE shortening in the western part of the block during extrusion, to account for the difference in sinistral displacement of 700 ± 200 km estimated for the northwestern part (Leloup et al., 1995) and 250 km for the southeastern part (Fig. 9c, Wang and Burchfiel, 1997) of the Ailao Shan-Red River fault. In Hall's (2002) model, E-W shortening in the western part of Indochina started at 32 Ma, and sinistral displacement along the Ailao Shan-Red River fault occurred at 32–16 Ma. From 15 Ma, there is ~50 km dextral displacement along the Ailao Shan-Red River fault. The Euler rotations of the Hall (2002) model predict a 3° clockwise rotation relative to South China, smaller than predicted by paleomagnetic data (Fig. 10a).

Replumaz and Tapponnier (2003) considered Indochina as a rigid block, and assumed a displacement of 745 km along the Ailao Shan-Red River fault at 30–15 Ma following the estimates of Leloup et al. (1995), Fig. 9b). From 5 Ma onwards they inferred a dextral displacement of 30 km (Replumaz et al., 2001). Their model predicts a 35° clockwise rotation from 40 Ma to present day, consistent with paleomagnetic data from Southern Simao, but much more than that of the Southern Indochina Block (Fig. 10a).

Royden et al. (2008) inferred a ~600 km sinistral motion on the Ailao Shan-Red River fault at the eastern part of the Vietnam block (Southern Indochina, Fig. 9d), which they considered as a rigid block contiguous with the rest of Indochina. They did not elaborate on how to reconcile this estimate with the 250 km sinistral displacement estimate by Wang and Burchfiel (1997). The western part of Indochina (their “Lanping-Simao unit”) is considered to have suffered major deformation and shortening after India-Asia collision and during Indochina extrusion, and therefore displacement along the northwestern section of the Ailao Shan-Red River fault may be even larger than ~600 km. The model predicts a 10° clockwise rotation of Indochina relative to the South China Block at 50–20 Ma, in reasonable agreement with paleomagnetic data from Southern Indochina (Fig. 10a).

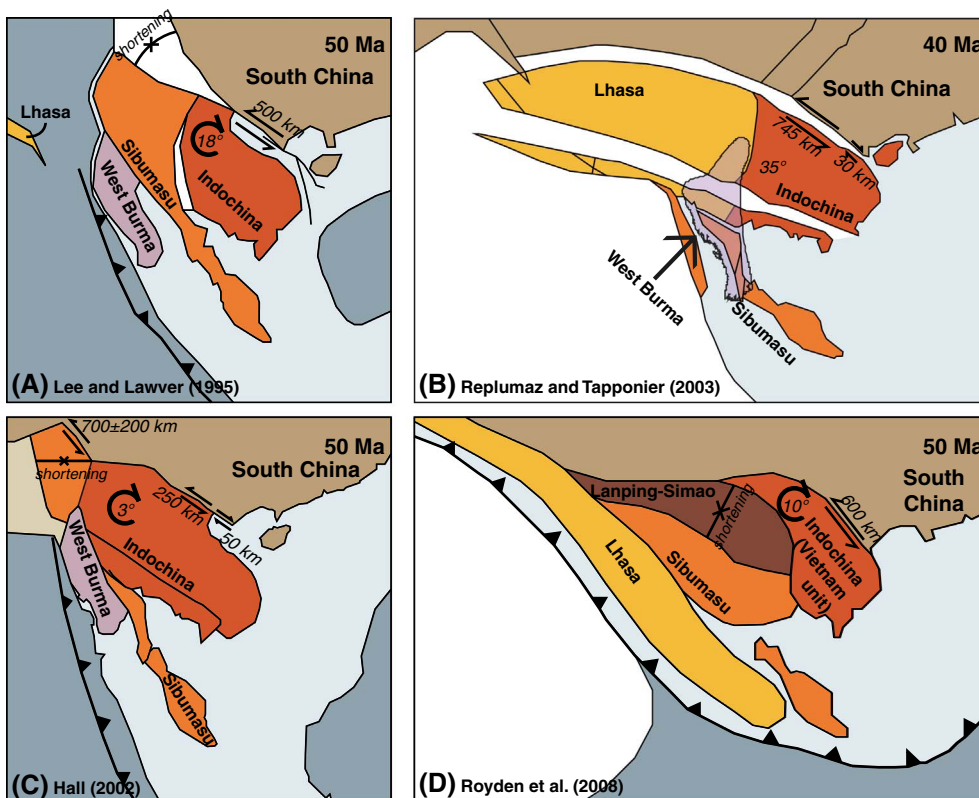


Fig. 9. Previous tectonic reconstructions of Indochina (A) Lee and Lawver (1995), (B) Replumaz and Tapponnier (2003), (C) Hall (2002), (D) Royden et al. (2008) that predicted different rotations of Indochina and displacements along the Ailao Shan-Red River fault. The outline of West Burma in Fig. 9(B) is following Hall et al. (2008). (For interpretation of the references to colour in this figure legend, the reader is referred to the web version of this article.)

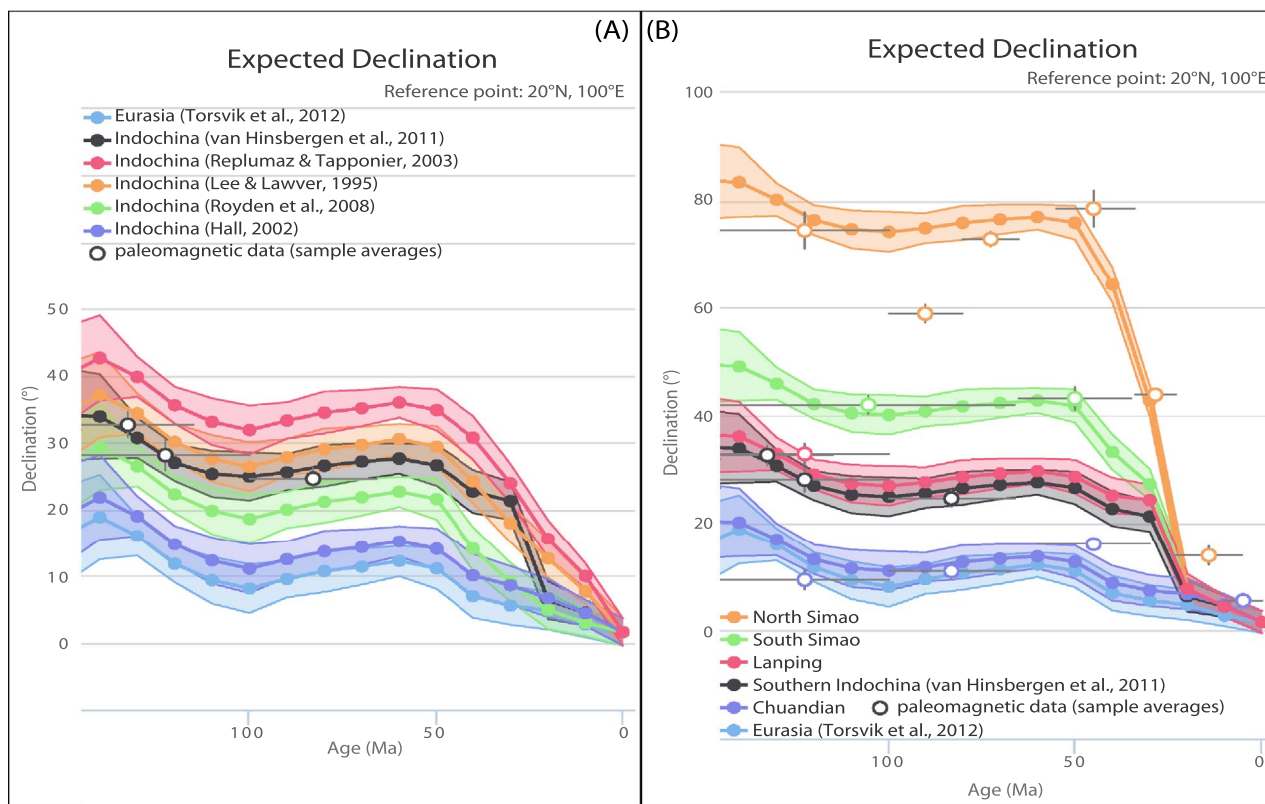


Fig. 10. Comparison of the predicted rotations by (A) previous reconstructions (Lee and Lawver, 1995; Hall, 2002; Replumaz and Tapponnier, 2003; Royden et al., 2008; van Hinsbergen et al., 2011a), (B) our reconstruction versus available paleomagnetic data. Note that the predicted rotations of different blocks by our reconstruction are consistent with the measured paleomagnetic data.

van Hinsbergen et al. (2011a) noticed different sinistral displacement estimates along the Ailao Shan-Red River fault of 250 km between 30 and 20 Ma (Searle, 2006; Hall et al., 2008; Fyhn et al., 2009) and ~700 km between 30 and 15 Ma (Tapponnier et al., 1982; Leloup et al., 1995), but struggled to reconcile how these estimates could be consistent with each other, because they considered Indochina as a rigid block. They adopted the smaller displacement estimate of 250 km between 30 and 20 Ma (Searle, 2006; Hall et al., 2008; Fyhn et al., 2009), followed by a 40 km dextral displacement from 8 Ma onwards, based on estimates by Fyhn et al. (2009), Replumaz et al. (2001), and Schoenbohm et al. (2006a). Their model predicted a 15° clockwise rotation of Indochina relative to the South China Block, consistent with paleomagnetic data (Fig. 10a).

In conclusion, most reconstructions assume rigidity of the Indochina Block, and fit the estimated amount of rotation of the Southern Indochina Block reasonably well. Even the high end of the predicted rotations of Replumaz and Tapponnier (2003), however, fails to predict major rotations and rotation differences recorded by paleomagnetic data in northwestern Indochina towards the SE margin of the Tibetan Plateau. In addition, current reconstructions tend to assume either the large or small end-member estimate for the Ailao Shan-Red River fault displacement, but do not reconcile these estimates. In the discussion below, we attempt a first-order reconstruction of the Indochina region that takes these rotation differences into account, and tests whether this may reconcile the different estimates of Ailao Shan-Red River fault displacement.

5.2.3. New reconstruction of Indochina deformation

Our new reconstruction aims to reconcile the paleomagnetic rotations with known faults in NW Indochina and estimates displacements of the NW Indochina blocks relative to the stable Southern Indochina domain that forms the stable, undeformed part of Southern Indochina.

The main reason that deformation within NW Indochina was previously not reconstructed in any detail is that little is known about Paleogene fault displacements and magnitude of deformation in this area. Our reconstruction is admittedly oversimplified, in that we assume that the paleomagnetically coherently rotating domains identified above are rigid blocks. The physiography and known geology of these blocks clearly indicate that many of them are internally intensely folded and thrust instead, and our assumption of block rigidity makes that the displacements that we estimate along faults that we assume as block boundaries are much higher than the currently available estimates. This discrepancy is likely at least in part explained by internal deformation of the blocks – a lateral variation of shortening within a region may also lead to coherent vertical axis rotations. On the other hand, the age and displacement of faults in NW Indochina are based on geomorphology, river bends across the faults, and fault bounded basins, accurate age constraints on these faults remain scarce. Therefore, the actual timing and displacement along these fault may be much older and larger than currently thought. For example, the Dien Bien Phu fault was previously thought to begin at 5 Ma (Lai et al., 2012), however, recent K-Ar age data on authigenic illite from the fault gouge samples indicates that the Dien Bien Phu fault began as early as Cretaceous and reactivated in the Oligocene (29–26 Ma, Bui et al., 2017).

Our reconstruction should be regarded as an attempt to quantify the horizontal motions accommodated within Indochina that caused the paleomagnetically constrained vertical axis rotations. With these simplifications in mind, we built our reconstruction of block rotations, and iteratively improved the reconstruction to become consistent with paleomagnetic data using the methodology outlined in Section 5.1 (Fig. 10b). This reconstruction assumes that the southern, stable Indochina Block underwent 250 km of sinistral displacement along the Ailao Shan-Red River fault relative to South China using the reconstruction of van Hinsbergen et al. (2011a) as basis, who followed estimates of Fyhn et al. (2009). We tested how much displacement was accommodated along the Ailao Shan-Red River fault in the northwest if

we assume that this fault was a pure strike-slip fault, and all NW Indochina blocks moved along this fault while rotating. Euler poles that describe the block motions are provided in Supplementary Information 3.

The NW Indochina-SE Tibetan Plateau margin is cut by a series of major Cenozoic faults that are incorporated in our reconstruction. The Xianshuihe-Xiaojiang fault separates Chuandian from South China and accommodated 78–100 km sinistral displacement from 13 Ma onwards (Roger et al., 1995; Zhang et al., 2004; Wang et al., 2009; Li et al., 2015). We infer that this fault accommodated 15° clockwise rotation of Chuandian relative to the South China Block (Fig. 8) and we adjust the reconstruction of Tibetan tectonics of van Hinsbergen et al. (2011a) to accommodate this rotation.

In the northwest of Indochina, we defined three terranes, Southern Simao, Northern Simao and Lanping, which are based on coherence in paleomagnetic data, and bounded by known faults (see Section 4.1, Figs. 2 and 4). We define the stable southeastern part of Indochina as the Southern Indochina Terrane. The Dien Bien Phu fault separates Southern Simao from the Southern Indochina (Lai et al., 2012). We infer 80 km rotation-related convergence and 175 km left-lateral slip between South Simao and Indochina along this fault at 50–17 Ma to accommodate 35° CW rotation relative to Indochina (Fig. 8). The Lancang fault separates Southern Simao from Northern Simao (Wang and Burchfiel, 1997; Wang et al., 2014). We infer 215 km rotation-related convergence between Southern Simao and Northern Simao along this fault at 50–20 Ma, to accommodate 50° CW rotation relative to Indochina. This is consistent with most available paleomagnetic data, except for the mid-Cretaceous (Fig. 10b). Mid-Cretaceous deformation is documented in Tibet (van Hinsbergen et al., 2011a), but is not reconstructed here. The Nanting River fault separates the Northern Simao from Lanping (Wang and Burchfiel, 1997; Lacassin et al., 1998, Fig. 8). Accommodating 50° difference in rotation between the Northern Simao and Lanping would require a large, 360 km sinistral motion along this fault if it had accommodated the entire rotation (but see the remarks on our assumptions above).

Restoring these block rotations culminates in a net NW-SE shortening in NW Indochina of as much as ~350 km. As a result, the assumption of 250 km of left-lateral slip along the Ailao Shan-Red River fault between the Southern Indochina Block and South China as suggested by Wang and Burchfiel (1997) and Fyhn et al. (2009) would result in a ~600 km sinistral displacement along this fault in northwestern Indochina (Fig. 8), consistent with the estimates of Leloup et al. (1995) and Chung et al. (1997). The rotations of Indochina may thus reconcile the long-standing discussion on the amount of extrusion from eastern Tibet. The large displacement along the northwestern part of the Ailao Shan-Red River fault requires greater shortening in northwestern Indochina, which is supported by previous geological study (Wang and Burchfiel, 1997).

Our first-order kinematic reconstruction incorporating the paleomagnetic results from the SE margin of the Tibetan Plateau and NW Indochina suggests that extrusion and shortening in the eastern Tibetan Plateau was more important than implied in the restoration of van Hinsbergen et al. (2011a). Our study suggests that their reconstruction may require an update to accommodate the larger amount of Indochina extrusion.

6. Conclusions

In this study, we reviewed all available paleomagnetic data from Indochina and South China blocks since Jurassic, and built a new reconstruction of Indochina deformation in Cenozoic based on the paleomagnetic data and geological observations. Our compilation shows that the extruding Indochina domain was not a rigid block, but that it contained major rotating blocks in particularly its northwestern parts. To facilitate the quantitative testing of kinematic restorations of block motions against paleomagnetic data, we provide a new tool on

the online paleomagnetic analysis platform Paleomagnetism.org that allows the prediction of the Global Apparent Polar Wander Path in the coordinates of any restored block, which can then be compared to paleomagnetic measurements from that block. Restoring the paleomagnetically constrained rotations of these blocks then shows that the northwestern parts of the Indochina domain extruded ~350 km farther to the southeast than the southeastern, stable Indochina Block. Assuming a ~250 km displacement of the Southern Indochina Block relative to South China along the Ailao Shan-Red River fault, as suggested by geological and geophysical studies, would yield ~600 km of extrusion of Indochina-related blocks from eastern Tibet, consistent with geological estimates from that region. Our reconstruction therefore provides the first reconciliation between paleomagnetic data and geological evidence from the Indochina Block. Contrary to earlier conclusions, we also find that paleomagnetic inclinations are inconsistent with a paleomagnetically significant southeastward motion of Indochina. Calculating paleolatitudes from the compiled inclinations would, when taken at face value, instead require major northward motions of Indochina and South China relative to Eurasia, which is in stark contrast with structural geological data. However, where inclination shallowing is correction for, inclinations coincide with those from Eurasia. We therefore suggest that these apparent motions are artifacts of compaction-induced inclination shallowing of the redbeds from which most of the paleomagnetic data were derived rather than tectonic motions.

Acknowledgements

Robert Hall is thanked for sharing his Euler poles of Indochina. We are grateful to reviews of Robert Hall and Ken Kodama who provided helpful comments. Financial assistance was provided by the National Natural Science Foundation of China grant 41404056 and the State Key Laboratory of Lithospheric Evolution grant 11431780. ELA and DJJvH were funded through ERC starting grant 306810 (SINK) and NWO VIDI grant 864.11.004. We thank Boris Gesbert for his help in building the paleomagnetic database.

Appendix A. Supplementary data

Supplementary data to this article can be found online at <http://dx.doi.org/10.1016/j.earscirev.2017.05.007>.

References

- Achache, J., Courtillot, V., Besse, J., 1983. Paleomagnetic constraints on the late Cretaceous and Cenozoic tectonics of southeastern Asia. *Earth Planet. Sci. Lett.* 63 (1), 123–136.
- Aihara, K., Takemoto, K., Zaman, H., Inokuchi, H., Miura, D., Surinkum, A., Paiyrom, A., Phajuy, B., Chantraprasert, S., Panjasawatwong, Y., Wongpornchai, P., Otofujii, Y., 2007. Internal deformation of the Shan-Thai block inferred from paleomagnetism of Jurassic sedimentary rocks in Northern Thailand. *J. Asian Earth Sci.* 30 (3–4), 530–541.
- Aitchison, J.C., Ali, J.R., Davis, A.M., 2007. When and where did India and Asia collide? *J. Geophys. Res.* B05423. <http://dx.doi.org/10.1029/2006JB004706>.
- Akciz, S., Burchfiel, B.C., Crowley, J.L., Yin, J., Chen, L., 2008. Geometry, kinematics, and regional significance of the Chong Shan shear zone, Eastern Himalayan Syntaxis, Yunnan, China. *Geosphere* 4 (1), 292–314.
- Allen, C., Gillespie, A.R., Han, Y., Sieh, K.E., Zhang, B.C., Zhu, C.N., 1984. Red River and associated faults, Yunnan Province, China - Quaternary geology, slip rates, and seismic hazard. *Geol. Soc. Am. Bull.* 95, 686–700.
- Barber, A.J., Crow, M.J., 2009. Structure of Sumatra and its implications for the tectonic assembly of Southeast Asia and the destruction of Paleotethys. *Island Arc* 18 (1), 3–20.
- Bertrand, G., Rangin, C., Maluski, H., Han, T.A., Thein, M., Myint, O., Maw, W., Lwin, S., 1999. Cenozoic metamorphism along the Shan scarp (Myanmar): evidences for ductile shear along the Sagaing fault or the northward migration of the eastern Himalayan syntaxis? *Geophys. Res. Lett.* 26 (7), 915–918.
- Bertrand, G., Rangin, C., Maluski, H., Bellon, H., 2001. Diachronous cooling along the Mogok Metamorphic Belt (Shan scarp, Myanmar): the trace of the northward migration of the Indian syntaxis. *J. Asian Earth Sci.* 19 (5), 649–659.
- Boyden, J.A., Müller, R.D., Gurnis, M., Torsvik, T.H., Clark, J.A., Turner, M., Ivey-Law, H., Watson, R.J., Cannon, J.S., 2011. Next-generation plate-tectonic reconstructions using GPlates. In: *Geoinformatics Cyberinfrastructure for the Solid Earth Sciences*, pp. 95–113.
- Briaïs, A., Patriat, P., Tapponnier, P., 1993. Updated interpretation of magnetic anomalies and seafloor spreading stages in the South China Sea: implications for the Tertiary tectonics of Southeast Asia. *J. Geophys. Res.* 98 (B4), 6299–6328.
- Bui, H.B., Ngo, X.T., Khuong, T.H., Golonka, J., Nguyen, T.D., Song, Y., Itaya, T., Yagi, K., 2017. Episodes of brittle deformation within the Dien Bien Phu Fault zone, Vietnam: evidence from K-Ar age dating of authigenic illite. *Tectonophysics* 695, 53–63.
- Butler, R.F., 1992. *Paleomagnetism: Magnetic Domains to Geologic Terranes*. Blackwell Scientific Publications, Boston (238pp).
- Cai, J.X., Zhang, K.J., 2009. A new model for the Indochina and South China collision during the Late Permian to the Middle Triassic. *Tectonophysics* 467 (1–4), 35–43.
- Cao, S., Liu, J.L., Leiss, B., Neubauer, F., Genser, J., Zhao, C.Q., 2011. Oligo-Miocene shearing along the Ailao Shan-Red River shear zone: constraints from structural analysis and zircon U/Pb geochronology of magmatic rocks in the Diancang Shan massif, SE Tibet, China. *Gondwana Res.* 19 (4), 975–993.
- Carter, A., Roques, D., Bristow, C., Kinny, P., 2001. Understanding Mesozoic accretion in Southeast Asia: significance of Triassic thermotectonism (Indosinian orogeny) in Vietnam. *Geology* 29 (3), 211–214.
- Chan, L.S., 1991. Paleomagnetism of Late Mesozoic granitic intrusions in Hong-Kong - implications for Upper Cretaceous reference pole of south China. *J. Geophys. Res.* Solid Earth Planets 96 (B1), 327–335.
- Charusiri, P., Imsamut, S., Zhuang, Z.H., Ampaiwan, T., Xu, X.X., 2006. Paleomagnetism of the earliest Cretaceous to early late Cretaceous sandstones, Khorat Group, Northeast Thailand: implications for tectonic plate movement of the Indochina block. *Gondwana Res.* 9 (3), 310–325.
- Charvet, J., 2013. The Neoproterozoic–Early Paleozoic tectonic evolution of the South China Block: an overview. *J. Asian Earth Sci.* 74, 198–209.
- Chen, H.H., Dobson, J., Heller, F., Hao, J., 1995. Paleomagnetic evidence for clockwise rotation of the Simao region since the Cretaceous: a consequence of India-Asia collision. *Earth Planet. Sci. Lett.* 134 (1–2), 203–217.
- Chi, C.T., Geissman, J.W., 2013. A review of the paleomagnetic data from Cretaceous to lower Tertiary rocks from Vietnam, Indochina and South China, and their implications for Cenozoic tectonism in Vietnam and adjacent areas. *J. Geodyn.* 69, 54–64.
- Chung, S.L., Lee, T.Y., Lo, C.H., Wang, P.L., Chen, C.Y., Yem, N.T., Hoa, T.T., Wu, G.Y., 1997. Intraplate extension prior to continental extrusion along the Ailao Shan Red River shear zone. *Geology* 25 (4), 311–314.
- Clark, M., Royden, L., Whipple, K., Burchfiel, B., Zhang, X., Tang, W., 2006. Use of a regional, relict landscape to measure vertical deformation of the eastern Tibetan Plateau. *J. Geophys. Res.* 111. <http://dx.doi.org/10.1029/2005JF00294>.
- Clift, P., Lee, G.H., Anh Duc, N., Barckhausen, U., Van Long, H., Zhen, S., 2008. Seismic reflection evidence for a dangerous grounds miniplate: no extrusion origin for the South China Sea. *Tectonics* 27 (3). <http://dx.doi.org/10.1029/2007tc002216>.
- Cogné, J.P., Kravchinsky, V.A., Halim, N., Hankard, F., 2005. Late Jurassic–Early Cretaceous closure of the Mongol–Okhotsk Ocean demonstrated by new Mesozoic palaeomagnetic results from the Trans-Baikal area (SE Siberia). *Geophys. J. Int.* 163 (2), 813–832.
- Copley, A., Avouac, J.P., Royer, J.-Y., 2010. India-Asia collision and the Cenozoic slowdown of the Indian plate: implications for the forces driving plate motions. *J. Geophys. Res.* 115 (B3). <http://dx.doi.org/10.1029/2009JB006634>.
- Curry, J.R., 2005. Tectonics and history of the Andaman Sea region. *J. Asian Earth Sci.* 25 (1), 187–232.
- Deenen, M., Langereis, C.G., van Hinsbergen, D.J.J., Biggin, A.J., 2011. Geomagnetic secular variation and the statistics of palaeomagnetic directions. *Geophys. J. Int.* 186 (2), 509–520.
- DeMets, C., Iaffaldano, G., Merkouriev, S., 2015. High-resolution Neogene and Quaternary estimates of Nubia-Eurasia-North America Plate motion. *Geophys. J. Int.* 203 (1), 416–427.
- Dupont-Nivet, G., Lippert, P.C., van Hinsbergen, D.J.J., Meijers, M.J.M., Kapp, P., 2010. Palaeolatitude and age of the Indo-Asia collision: palaeomagnetic constraints. *Geophys. J. Int.* 182, 1189–1198.
- Enkin, R.J., Yang, Z., Chen, Y., Courtillot, V., 1992. Paleomagnetic constraints on the geodynamic history of the major blocks of China from the Permian to the present. *J. Geophys. Res.* 97 (B10), 13953–13989.
- Fang, W., Van der Voo, R., Liang, Q., 1989. Devonian paleomagnetism of Yunnan Province across the Shan Thai-South China suture. *Tectonics* 8 (5), 939–952.
- Faure, M., Lepvrier, C., Nguyen, V.V., Vu, T.V., Lin, W., Chen, Z., 2014. The South China block-Indochina collision: where, when, and how? *J. Asian Earth Sci.* 79, 260–274.
- Fisher, R., 1953. Dispersion on a sphere. In: *Proceedings of the Royal Society of London. Series A. Mathematical and Physical Sciences*, 217 1130. pp. 295–305.
- Fujiwara, K.P., Zaman, H., Surinkum, A., Chaiwong, N., Fujihara, M., Ahn, H.S., Otofujii, Y., 2014. New insights into regional tectonics of the Indochina Peninsula inferred from Lower-Middle Jurassic paleomagnetic data of the Sibumasu Terrane. *J. Asian Earth Sci.* 94, 126–138.
- Funahara, S., Nishiwaki, N., Miki, M., Murata, F., Otofujii, Y., Wang, Y.Z., 1992. Paleomagnetic study of Cretaceous rocks from the Yangtze block, central Yunnan, China: implications for the India-Asia collision. *Earth Planet. Sci. Lett.* 113 (1–2), 77–91.
- Funahara, S., Nishiwaki, N., Murata, F., Otofujii, Y., Wang, Y.Z., 1993. Clockwise rotation of the Red River fault inferred from paleomagnetic study of Cretaceous rocks in the Shan-Thai-Malay block of Western Yunnan, China. *Earth Planet. Sci. Lett.* 117 (1–2), 29–42.
- Fyhn, M., Boldreel, L.O., Nielsen, L.H., 2009. Geological development of the Central and South Vietnamese margin: implications for the establishment of the South China Sea, Indochinese escape tectonics and Cenozoic volcanism. *Tectonophysics* 478 (3–4),

- 184–214.
- Gan, W., Zhang, P., Shen, Z.K., Niu, Z., Wang, M., Wan, Y., Zhou, D., Cheng, J., 2007. Present-day crustal motion within the Tibetan plateau inferred from GPS measurements. *J. Geophys. Res.* 112 (B8), 582–596.
- Gao, L., Yang, Z., Tong, Y., Wang, H., An, C., 2015. New paleomagnetic studies of Cretaceous and Miocene rocks from Jinggu, western Yunnan, China: evidence for internal deformation of the Lanping–Simao Terrane. *J. Geodyn.* 89, 39–59.
- Gilder, S., Courtillot, V., 1997. Timing of the North-South China collision from new middle to late Mesozoic paleomagnetic data from the North China Block. *J. Geophys. Res.* 102 (B8), 17713–17727.
- Gilder, S., Chen, Y., Sen, S., 2001. Oligo-Miocene magnetostratigraphy and rock magnetism of the Xishuigou section, Subei (Gansu Province, western China) and implications for shallow inclinations in central Asia. *J. Geophys. Res.* 106 (12), 30505–30522.
- Gilley, L., 2003. Direct dating of left-lateral deformation along the Red River shear zone, China and Vietnam. *J. Geophys. Res.* 108 (B2). <http://dx.doi.org/10.1029/2001jb001726>.
- Hall, R., 2002. Cenozoic geological and plate tectonic evolution of SE Asia and the SW Pacific: computer-based reconstructions, model and animations. *J. Asian Earth Sci.* 20 (4), 353–431.
- Hall, R., van Hattum, M.W.A., Spakman, W., 2008. Impact of India-Asia collision on SE Asia: the record in Borneo. *Tectonophysics* 451 (1–4), 366–389.
- Hu, X., Garzanti, E., Moore, T., Raffi, I., 2015. Direct stratigraphic dating of India-Asia collision onset at the Selandian (middle Paleocene, 59 ± 1 Ma). *Geology* 43 (10), 859–862.
- Hu, X., Garzanti, E., Wang, J., Huang, W., An, W., Webb, A., 2016. The timing of India-Asia collision onset – facts, theories, controversies. *Earth Sci. Rev.* 160, 264–299.
- Huang, K., Opdyke, N.D., 1991a. Paleomagnetic results from the Upper Carboniferous of the Shan-Thai-Malay block of western Yunnan, China. *Tectonophysics* 192 (3–4), 333–344.
- Huang, K., Opdyke, N.D., 1992. Paleomagnetism of Cretaceous to lower Tertiary rocks from southwestern Sichuan: a revisit. *Earth Planet. Sci. Lett.* 112 (1–4), 29–40.
- Huang, K., Opdyke, N.D., 1993. Paleomagnetic results from Cretaceous and Jurassic rocks of South and Southwest Yunnan: evidence for large clockwise rotations in the Indochina and Shan-Thai-Malay terranes. *Earth Planet. Sci. Lett.* 117 (3–4), 507–524.
- Huang, K., Opdyke, N.D., 2015. Post-folding magnetization of the Triassic rocks from western Guizhou and southern Yunnan provinces: new evidence for large clockwise rotations in the Simao Terrane. *Earth Planet. Sci. Lett.* 423, 155–163.
- Huang, B.C., Zhou, Y.X., Zhu, R.X., 2008. Discussions on Phanerozoic evolution and formation of continental China, based on paleomagnetic studies (in Chinese). *Earth Sci. Front.* 15 (3), 348–359.
- Huang, S., Pan, Y., Zhu, R., 2012. Paleomagnetism of the Late Cretaceous volcanic rocks of the Shimaoshan Group in Yongtai County, Fujian Province. *Science in China, Series D* 56 (1), 22–30.
- Huang, W., Dupont-Nivet, G., Lippert, P.C., van Hinsbergen, D.J.J., Hallot, E., 2013. Inclination shallowing in Eocene Linnizong sedimentary rocks from Southern Tibet: correction, possible causes and implications for reconstructing the India-Asia collision. *Geophys. J. Int.* 194 (3), 1390–1411.
- Huang, W., van Hinsbergen, D.J.J., Maffione, M., Orme, D.A., Dupont-Nivet, G., Guilmette, C., Ding, L., Guo, Z., Kapp, P., 2015. Lower Cretaceous Xigaze ophiolites formed in the Gangdese forearc: evidence from paleomagnetism, sediment provenance, and stratigraphy. *Earth Planet. Sci. Lett.* 415, 142–153.
- Ingalls, M., Rowley, D.B., Currie, B., Colman, A.S., 2016. Large-scale subduction of continental crust implied by India-Asia mass-balance calculation. *Nat. Geosci.* 9 (11), 848–853.
- Jagoutz, O., Royden, L., Holt, A.F., Becker, T.W., 2015. Anomalously fast convergence of India and Eurasia caused by double subduction. *Nat. Geosci.* 8 (6), 475–478.
- Jian, P., Liu, D., Kröner, A., Zhang, Q., Wang, Y., Sun, X., Zhang, W., 2009. Devonian to Permian plate tectonic cycle of the Paleo-Tethys Orogen in southwest China (II): insights from zircon ages of ophiolites, arc/back-arc assemblages and within-plate igneous rocks and generation of the Emeishan CFB province. *Lithos* 113 (3–4), 767–784.
- Johnson, C.L., Constable, C.G., Tauxe, L., Barendregt, R., Brown, L.L., Coe, R.S., Layer, P., Mejia, V., Opdyke, N.D., Singer, B.S., Staudigel, H., Stone, D.B., 2008. Recent investigations of the 0–5 Ma geomagnetic field recorded by lava flows. *Geochem. Geophys. Geosyst.* 9 (4). <http://dx.doi.org/10.1029/2007GC001696>.
- King, R.F., 1955. The remanent magnetism of artificially deposited sediments. *Geophys. J. Int.* 7 (Suppl.3), 115–134.
- Kodama, K.P., 2012. Paleomagnetism of Sedimentary Rocks: Process and Interpretation. John Wiley & Sons, Ltd, Oxford (253 pp).
- Kodama, K.P., Sun, W.W., 1992. Magnetic anisotropy as a correction for compaction-caused palaeomagnetic inclination shallowing. *Geophys. J. Int.* 111, 465–469.
- Kondo, K., Mu, C.L., Yamamoto, T., Zaman, H., Miura, D., Yokoyama, M., Ahn, H.S., Otofujii, Y., 2012. Oroclinal origin of the Simao Arc in the Shan-Thai Block inferred from the Cretaceous palaeomagnetic data. *Geophys. J. Int.* 190 (1), 201–216.
- Kornfeld, D., Eckert, S., Appel, E., Ratschbacher, L., Pfänder, J., Liu, D., 2014a. Clockwise rotation of the Baoshan Block due to southeastward tectonic escape of Tibetan crust since the Oligocene. *Geophys. J. Int.* 197 (1), 149–163.
- Kornfeld, D., Eckert, S., Appel, E., Ratschbacher, L., Sonntag, B.L., Pfänder, J.A., Ding, L., Liu, D.L., 2014b. Cenozoic clockwise rotation of the Tengchong block, southeastern Tibetan Plateau: a paleomagnetic and geochronologic study. *Tectonophysics* 628, 105–122.
- Kornfeld, D., Sonntag, B.-L., Gast, S., Matthes, J., Ratschbacher, L., Pfänder, J.A., Eckert, S., Liu, D., Appel, E., Ding, L., 2014c. Apparent paleomagnetic rotations reveal Pliocene–Holocene internal deformation of the Tengchong Block, southeastern Tibetan Plateau. *J. Asian Earth Sci.* 96 (0), 1–16.
- Koymans, M.R., Langereis, C.G., Pastor-Galán, D., van Hinsbergen, D.J.J., 2016. Paleomagnetism.org: an online multi-platform open source environment for paleomagnetic data analysis. *Comput. Geosci.* 93, 127–137.
- Lacassin, R., Maluski, H., Leloup, P.H., Tapponnier, P., Hinthong, C., Siribhakdi, K., Chuaviroj, S., Charoenravat, A., 1997. Tertiary diachronic extrusion and deformation of western Indochina: structural and Ar-40/Ar-39 evidence from NW Thailand. *J. Geophys. Res.* 102 (B5), 10013–10037.
- Lacassin, R., Replumaz, A., Leloup, P.H., 1998. Hairpin river loops and slip-sense inversion on southeast Asian strike-slip faults. *Geology* 26 (8), 703–706.
- Lai, K.Y., Chen, Y.G., Lâm, D.D., 2012. Pliocene-to-present morphotectonics of the Dien Bien Phu fault in northwest Vietnam. *Geomorphology* 173–174, 52–68.
- Lee, T.Y., Lawver, L.A., 1995. Cenozoic plate reconstruction of Southeast Asia. *Tectonophysics* 251 (1–4), 85–138.
- Leech, M.L., Singh, S., Jain, A.K., Klemperer, S.L., Manickavasagam, R.M., 2005. The onset of UHP-Asia continental collision: early, steep subduction required by the timing of UHP metamorphism in the western Himalaya. *Earth Planet. Sci. Lett.* 234 (1–2), 83–97.
- Leloup, P., Harrison, T.M., Ryerson, F., Wenji, C., Qi, L., Tapponnier, P., Lacassin, R., 1993. Structural, petrological and thermal evolution of a Tertiary ductile strike-slip shear zone, Diancang Shan, Yunnan. *J. Geophys. Res.* 98 (B4), 6715–6743.
- Leloup, P., Lacassin, R., Tapponnier, P., Schärer, U., Zhong, D.L., Liu, X.H., Zhang, L.S., Ji, S.C., Trinh, P.T., 1995. The Ailao Shan-Red River shear zone (Yunnan, China), Tertiary transform boundary of Indochina. *Tectonophysics* 251 (1–4), 3–84.
- Leloup, P.H., Arnaud, N., Lacassin, R., Kienast, J.R., Harrison, T.M., Trong, T.T.P., Replumaz, A., Tapponnier, P., 2001. New constraints on the structure, thermochronology, and timing of the Ailao Shan-Red River shear zone, SE Asia. *J. Geophys. Res.* 106 (B4), 6683–6732.
- Li, Y., Ali, J.R., Chan, L.S., Lee, C.M., 2005. New and revised set of Cretaceous paleomagnetic poles from Hong Kong: implications for the development of southeast China. *J. Asian Earth Sci.* 24 (4), 481–493.
- Li, X.H., Li, W.X., Li, Z.X., Lo, C.H., Wang, J., Ye, M.F., Yang, Y.H., 2009. Amalgamation between the Yangtze and Cathaysia Blocks in South China: constraints from SHRIMP U–Pb zircon ages, geochemistry and Nd–Hf isotopes of the Shuangxiwu volcanic rocks. *Precambrian Res.* 174 (1–2), 117–128.
- Li, S.H., Huang, B.C., Zhu, R.X., 2012. Paleomagnetic constrains on the tectonic rotation of the southeastern margin of the Tibetan Plateau. *Chin. J. Geophys.* 55 (1), 76–94.
- Li, S.H., Deng, C.L., Yao, H.T., Huang, S., Liu, C.Y., He, H.Y., Pan, Y.X., Zhu, R.X., 2013a. Magnetostratigraphy of the Dali Basin in Yunnan and implications for late Neogene rotation of the southeast margin of the Tibetan Plateau. *J. Geophys. Res.* 118 (3), 791–807.
- Li, Y.X., Shu, L., Wen, B., Yang, Z., Ali, J.R., 2013b. Magnetic inclination shallowing problem and the issue of Eurasia's rigidity: insights following a palaeomagnetic study of upper Cretaceous basalts and redbeds from SE China. *Geophys. J. Int.* 194, 1374–1389.
- Li, S.H., Deng, C.L., Dong, W., Sun, L., Liu, S.Z., Qin, H.F., Yin, J.Y., Ji, X.P., Zhu, R.X., 2015. Magnetostratigraphy of the Xiaolongtan Formation bearing *Lufengipterus keiyuanensis* in Yunnan, southwestern China: constraint on the initiation time of the southern segment of the Xianshuihe-Xiaojiang fault. *Tectonophysics* 655, 213–226.
- Li, S.H., Yang, Z., Deng, C., He, H., Qin, H., Sun, L., Yuan, J., van Hinsbergen, D.J.J., Krijgsman, W., Dekkers, M.J., Pan, Y., Zhu, R., 2017. Clockwise rotations recorded in redbeds from the Jinggu Basin of northwestern Indochina. *Geol. Soc. Am. Bull.* <http://dx.doi.org/10.1130/B31637>.
- Lin, T.H., Lo, C.H., Chung, S.L., Hsu, F.J., Yeh, M.W., Lee, T.Y., Ji, J.Q., Wang, Y.Z., Liu, D., 2009. $^{40}\text{Ar}/^{39}\text{Ar}$ dating of the Jiali and Gaoligong shear zones: implications for crustal deformation around the Eastern Himalayan Syntaxis. *J. Asian Earth Sci.* 34 (5), 674–685.
- Lippert, P., van Hinsbergen, D., Dupont-Nivet, G., 2014. Early Cretaceous to present latitude of the central proto-Tibetan Plateau: a paleomagnetic synthesis with implications for Cenozoic tectonics, paleogeography, and climate of Asia. In: Nie, J., Hoke, G.D., Horton, B.K. (Eds.), *Toward an Improved Understanding of Uplift Mechanisms and the Elevation History of the Tibetan Plateau*. Geological Society of America Special Paper 507 [http://dx.doi.org/10.1130/2014.2507\(01\)](http://dx.doi.org/10.1130/2014.2507(01)).
- Liu, Y.Y., Morinaga, H., 1999. Cretaceous palaeomagnetic results from Hainan Island in south China supporting the extrusion model of Southeast Asia. *Tectonophysics* 301 (1–2), 133–144.
- Liu, J., Tang, Y., Tran, M.D., Cao, S.Y., Zhao, L., Zhang, Z.C., Zhao, Z.D., Chen, W., 2012. The nature of the Ailao Shan-Red River (ASRR) shear zone: constraints from structural, microstructural and fabric analyses of metamorphic rocks from the Diancang Shan, Ailao Shan and Day Nui Con Voi massifs. *J. Asian Earth Sci.* 47, 231–251.
- Liu-Zeng, J., Tapponnier, P., Gaudemer, Y., Ding, L., 2008. Quantifying landscape differences across the Tibetan plateau: implications for topographic relief evolution. *J. Geophys. Res.* 113 (F4). <http://dx.doi.org/10.1029/2007JF000897>.
- Ma, Y., Yang, T., Yang, Z., Zhang, S., Wu, H., Li, H., Li, H., Chen, W., Zhang, J., Ding, J., 2014. Paleomagnetism and U–Pb zircon geochronology of lower Cretaceous lava flows from the western Lhasa terrane: new constraints on the India-Asia collision process and intracontinental deformation within Asia. *J. Geophys. Res.* 119 (10), 7404–7424.
- Maranate, S., Vella, P., 1986. Paleomagnetism of the Khorat Group, Mesozoic, Northeast Thailand. *J. SE Asian Earth Sci.* 1 (1), 23–31.
- Mazur, S., Green, C., Stewart, M.G., Whittaker, J.M., Williams, S., Bouatmani, R., 2012. Displacement along the Red River Fault constrained by extension estimates and plate reconstructions. *Tectonics* 31 (5). <http://dx.doi.org/10.1029/2012tc003174>.
- McElhinny, M.W., Embleton, B.J.J., Ma, X.H., Zhang, Z.K., 1981. Fragmentation of Asia in the Permian. *Nature* 293 (5829), 212–216.
- Meng, Q.R., Zhang, G.W., 1999. Timing of collision of the north and South China blocks:

- controversy and reconciliation. *Geology* 27 (2), 123–126.
- Metcalfe, I., 1996. Pre-Cretaceous evolution of SE Asian terranes. *Geol. Soc. Lond., Spec. Publ.* 106 (1), 97–122.
- Metcalfe, I., 2002. Permian tectonic framework and palaeogeography of SE Asia. *J. Asian Earth Sci.* 20 (6), 551–566.
- Metcalfe, I., 2013. Gondwana dispersion and Asian accretion: tectonic and palaeogeographic evolution of eastern Tethys. *J. Asian Earth Sci.* 66, 1–33.
- Mitchell, A.H.G., 1993. Cretaceous-Cenozoic tectonic events in the western Myanmar (Burma) Assam region. *J. Geol. Soc.* 150, 1089–1102.
- Molnar, P., Stock, J.M., 2009. Slowing of India's convergence with Eurasia since 20 Ma and its implications for Tibetan mantle dynamics. *Tectonics* 28, TC3001. <http://dx.doi.org/10.1029/2008TC002271>.
- Molnar, P., Tapponnier, P., 1975. Cenozoic tectonics of Asia: effects of a continental collision: features of recent continental tectonics in Asia can be interpreted as results of the India-Eurasia collision. *Science* 189 (4201), 419–426.
- Morinaga, H., Liu, Y.Y., 2004. Cretaceous paleomagnetism of the eastern South China Block: establishment of the stable body of SCB. *Earth Planet. Sci. Lett.* 222 (3–4), 971–988.
- Morley, C.K., 2007. Variations in Late Cenozoic–recent strike-slip and oblique-extensional geometries, within Indochina: the influence of pre-existing fabrics. *J. Struct. Geol.* 29 (1), 36–58.
- Najman, Y., Appel, E., Boudagher-Fadel, M., Bown, P., Carter, A., Garzanti, E., Godin, L., Han, J., Liebke, U., Oliver, G., Parrish, R., Vezzoli, G., 2010. Timing of India-Asia collision: geological, biostratigraphic, and palaeomagnetic constraints. *J. Geophys. Res.* B12416. <http://dx.doi.org/10.1029/2010JB007673>.
- Narumoto, K., Yang, Z., Takemoto, K., Zaman, H., Morinaga, H., Otofujii, Y.-i., 2006. Anomalously shallow inclination in middle-northern part of the South China block: palaeomagnetic study of Late Cretaceous red beds from Yichang area. *Geophys. J. Int.* 164 (2), 290–300.
- Orme, D.A., Carrapa, B., Kapp, P., 2014. Sedimentology, provenance and geochronology of the upper Cretaceous–lower Eocene western Xigaze forearc basin, southern Tibet. *Basin Res.* 27, 387–411.
- Otofujii, Y., Inoue, Y., Funahara, S., Murata, F., Zheng, X., 1990. Palaeomagnetic study of eastern Tibet—deformation of the Three Rivers region. *Geophys. J. Int.* 103 (1), 85–94.
- Otofujii, Y., Liu, Y., Yokoyama, M., Tamai, M., Yin, J., 1998. Tectonic deformation of the southwestern part of the Yangtze craton inferred from paleomagnetism. *Earth Planet. Sci. Lett.* 156 (1–2), 47–60.
- Otofujii, Y., Yokoyama, M., Kitada, K., Zaman, H., 2010. Paleomagnetic versus GPS determined tectonic rotation around eastern Himalayan syntaxis in East Asia. *J. Asian Earth Sci.* 37 (5–6), 438–451.
- Otofujii, Y., Tung, V.D., Fujihara, M., Tanaka, M., Yokoyama, M., Kitada, K., Zaman, H., 2012. Tectonic deformation of the southeastern tip of the Indochina Peninsula during its southward displacement in the Cenozoic time. *Gondwana Res.* 22 (2), 615–627.
- Replumaz, A., Tapponnier, P., 2003. Reconstruction of the deformed collision zone between India and Asia by backward motion of lithospheric blocks. *J. Geophys. Res.* Solid Earth 108 (B6). <http://dx.doi.org/10.1029/2001jb000661>.
- Replumaz, A., Lacassin, R., Tapponnier, P., Leloup, P., 2001. Large river offsets and Plio-Quaternary dextral slip rate on the Red River fault (Yunnan, China). *J. Geophys. Res.* 106 (B1), 819–836.
- Richter, B., Fuller, M., 1996. Palaeomagnetism of the Sibumasu and Indochina Blocks: Implications for the Extrusion Tectonic Model. *Tectonic Evolution of Southeast Asia*, 106. Geological Society, London, Special Publications, London (203–224 pp).
- Roger, F., Calassou, S., Lancelot, J., Malavieille, J., Mattauer, M., Xu, Z.Q., Hao, Z.W., Hou, L.W., 1995. Miocene emplacement and deformation of the Qong-Shan granite (Xiashui-He fault zone, West Sichuan, China) - geodynamic implications. *Earth Planet. Sci. Lett.* 130 (1–4), 201–216.
- Royden, L., Burchfiel, B.C., van der Hilst, R.D., 2008. The geological evolution of the Tibetan plateau. *Science* 321 (5892), 1054–1058.
- Sato, K., Liu, Y., Zhu, Z., Yang, Z., Otofujii, Y.-i., 1999. Paleomagnetic study of middle Cretaceous rocks from Yunlong, western Yunnan, China: evidence of southward displacement of Indochina. *Earth Planet. Sci. Lett.* 165 (1), 1–15.
- Sato, K., Liu, Y.Y., Zhu, Z.C., Yang, Z.Y., Otofujii, Y., 2001. Tertiary paleomagnetic data from northwestern Yunnan, China: further evidence for large clockwise rotation of the Indochina block and its tectonic implications. *Earth Planet. Sci. Lett.* 185 (1–2), 185–198.
- Sato, K., Liu, Y.Y., Wang, Y.B., Yokoyama, M., Yoshioka, S., Yang, Z., Otofujii, Y.I., 2007. Paleomagnetic study of Cretaceous rocks from Pu'er, western Yunnan, China: evidence of internal deformation of the Indochina block. *Earth Planet. Sci. Lett.* 258 (1–2), 1–15.
- Schärer, U., Tapponnier, P., Lacassin, R., Leloup, P.H., Dalai, Z., Ji, S.C., 1990. Intraplate tectonics in Asia - a precise age for large-scale Miocene movement along the Ailao-Shan-Red-River shear zone, China. *Earth Planet. Sci. Lett.* 97 (1–2), 65–77.
- Schärer, U., Zhang, L.-S., Tapponnier, P., 1994. Duration of strike-slip movements in large shear zones: the Red River belt, China. *Earth Planet. Sci. Lett.* 126 (4), 379–397.
- Schoenbohm, L., Burchfiel, B.C., Chen, L., Yin, J., 2006a. Miocene to present activity along the Red River fault, China, in the context of continental extrusion, upper-crustal rotation, and lower-crustal flow. *Geol. Soc. Am. Bull.* 118 (5–6), 672–688.
- Schoenbohm, L., Burchfiel, B.C., Chen, L.Z., 2006b. Propagation of surface uplift, lower crustal flow, and Cenozoic tectonics of the southeast margin of the Tibetan Plateau. *Geology* 34 (10), 813–816.
- Searle, M., 2006. Role of the Red River shear zone, Yunnan and Vietnam, in the continental extrusion of SE Asia. *J. Geol. Soc.* 163, 1025–1036.
- Searle, M.P., Noble, S.R., Cottle, J.M., Waters, D.J., Mitchell, A.H.G., Hlaing, T., Horstwood, M.S.A., 2007. Tectonic evolution of the Mogok metamorphic belt, Burma (Myanmar) constrained by U-Th-Pb dating of metamorphic and magmatic rocks. *Tectonics* 26 (3). <http://dx.doi.org/10.1029/2006tc002083>.
- Searle, M., Yeh, M.W., Lin, T.H., Chung, S.L., 2010. Structural constraints on the timing of left-lateral shear along the Red River shear zone in the Ailao Shan and Diancang Shan Ranges, Yunnan, SW China. *Geosphere* 6 (4), 316–338.
- Şengör, A.C., 1984. The Cimmeride orogenic system and the tectonics of Eurasia. *Geol. Soc. Am. Spec. Pap.* 195, 1–74.
- Seton, M., Müller, R.D., Zahirovic, S., Gaina, C., Torsvik, T.H., Shephard, G., Talsma, A., Gurnis, M., Turner, M., Maus, S., Chandler, M., 2012. Global continental and ocean basin reconstructions since 200 Ma. *Earth Sci. Rev.* 113 (3–4), 212–270.
- Sevastjanova, I., Hall, R., Rittner, M., Paw, S.M.T.L., Naing, T.T., Alderton, D.H., Comfert, G., 2016. Myanmar and Asia united, Australia left behind long ago. *Gondwana Res.* 32, 24–40.
- Socquet, A., Pubellier, M., 2005. Cenozoic deformation in western Yunnan (China–Myanmar border). *J. Asian Earth Sci.* 24 (4), 495–515.
- Sone, M., Metcalfe, I., 2008. Parallel Tethyan sutures in mainland Southeast Asia: new insights for Palaeo-Tethys closure and implications for the Indosinian orogeny. *Compt. Rendus Geosci.* 340 (2), 166–179.
- Sun, Z.M., Yang, Z., Yang, T., Pei, J., Yu, Q., 2006. New Late Cretaceous and Paleogene paleomagnetic results from south China and their geodynamic implications. *J. Geophys. Res.* 111 (B3). <http://dx.doi.org/10.1029/2004jb003455>.
- Sun, Z.M., Jiang, W., Li, H.B., Pei, J.L., Zhu, Z.M., 2010. New paleomagnetic results of Paleocene volcanic rocks from the Lhasa block: tectonic implications for the collision of India and Asia. *Tectonophysics* 490, 257–266.
- Takemoto, K., Halim, N., Otofujii, Y., Van Tri, T., Van De, L., Hada, S., 2005. New paleomagnetic constraints on the extrusion of Indochina: Late Cretaceous results from the Song Da terrane, northern Vietnam. *Earth Planet. Sci. Lett.* 229 (3–4), 273–285.
- Takemoto, K., Sato, S., Chanthavichith, K., Inthavong, T., Inokuchi, H., Fujihara, M., Zaman, H., Yang, Z., Yokoyama, M., Iwamoto, H., Otofujii, Y., 2009. Tectonic deformation of the Indochina Peninsula recorded in the Mesozoic palaeomagnetic results. *Geophys. J. Int.* 179 (1), 97–111.
- Tamai, M., Liu, Y.Y., Lu, L.Z., Yokoyama, M., Halim, N., Zaman, H., Otofujii, Y., 2004. Palaeomagnetic evidence for southward displacement of the Chuan Dian fragment of the Yangtze Block. *Geophys. J. Int.* 158 (1), 297–309.
- Tan, X., Kodama, K.P., Chen, H., Fang, D., Sun, D., Li, Y., 2003. Paleomagnetism and magnetic anisotropy of Cretaceous red beds from the Tarim basin, northwest China: evidence for a rock magnetic cause of anomalously shallow paleomagnetic inclinations from central Asia. *J. Geophys. Res.* 108 (B2). <http://dx.doi.org/10.1029/2001jb001608>.
- Tanaka, K., Mu, C., Sato, K., Takemoto, K., Miura, D., Liu, Y., Zaman, H., Yang, Z., Yokoyama, M., Iwamoto, H., Uno, K., Otofujii, Y., 2008. Tectonic deformation around the eastern Himalayan syntaxis: constraints from the Cretaceous palaeomagnetic data of the Shan-Thai Block. *Geophys. J. Int.* 175 (2), 713–728.
- Tapponnier, P., Peltzer, G., Le Dain, A.Y., Armijo, R., Cobbold, P., 1982. Propagating extrusion tectonics in Asia: new insights from simple experiments with plasticine. *Geology* 10 (12), 611–616.
- Tapponnier, P., Lacassin, R., Leloup, P.H., Scharer, U., Zhong, D.L., Wu, H.W., Liu, X.H., Ji, S.C., Zhang, L.S., Zhong, J.Y., 1990. The Ailao Shan Red River metamorphic belt - Tertiary left-lateral shear between Indochina and South China. *Nature* 343 (6257), 431–437.
- Tapponnier, P., Zhiqin, X., Roger, F., Meyer, B., Arnaud, N., Wittlinger, G., Jingsui, Y., 2001. Oblique stepwise rise and growth of the Tibet plateau. *Science* 294 (5547), 1671–1677.
- Tauxe, L., 2005. Inclination flattening and the geocentric axial dipole hypothesis. *Earth Planet. Sci. Lett.* 233 (3–4), 247–261.
- Tauxe, L., Kent, D.V., 2004. A simplified statistical model for the geomagnetic field and the detection of shallow bias in paleomagnetic inclinations: was the ancient magnetic field dipolar? In: Channell, J.E.T., Kent, D.V., Lowrie, W., Meert, J.G. (Eds.), *Timescales of the Paleomagnetic Field*. *Geophys. Monogr. Ser.*, Vol. 145 American Geophysical Union, Washington, D.C., pp. 101–115.
- Tong, Y.B., Yang, Z., Zheng, L.D., Xu, Y.L., Wang, H., Gao, L., Hu, X.Z., 2013. Internal crustal deformation in the northern part of Shan-Thai Block: new evidence from paleomagnetic results of Cretaceous and Paleogene redbeds. *Tectonophysics* 608, 1138–1158.
- Tong, Y.B., Yang, Z., Wang, H., Gao, L., An, C.-Z., Zhang, X.D., Xu, Y.C., 2015. The Cenozoic rotational extrusion of the Chuan Dian Fragment: new paleomagnetic results from Paleogene red-beds on the southeastern edge of the Tibetan Plateau. *Tectonophysics* 658, 46–60.
- Tong, Y.B., Yang, Z., Jing, X., Zhao, Y., Li, C., Huang, D., Zhang, X., 2016. New insights into the Cenozoic lateral extrusion of crustal blocks on the southeastern edge of Tibetan Plateau: evidence from paleomagnetic results from Paleogene sedimentary strata of the Baoshan Terrane. *Tectonics* 35 (11), 2494–2514. <http://dx.doi.org/10.1002/2016TC004221>.
- Torsvik, T.H., Van der Voo, R., Preeden, U., Mac Niocaill, C., Steinberger, B., Doubrovine, P.V., van Hinsbergen, D.J.J., Domeier, M., Gaina, C., Tohver, E., Meert, J.G., McCausland, P.J.A., Cocks, L.R.M., 2012. Phanerozoic polar wander, palaeogeography and dynamics. *Earth Sci. Rev.* 114 (3–4), 325–368.
- Tsuchiyama, Y., Zaman, H., Sotham, S., Samuth, Y., Sato, E., Ahn, H.-S., Uno, K., Tsumura, K., Miki, M., Otofujii, Y., 2016. Paleomagnetism of Late Jurassic to Early Cretaceous red beds from the Cardamom Mountains, southwestern Cambodia: tectonic deformation of the Indochina Peninsula. *Earth Planet. Sci. Lett.* 434, 274–288.
- Tsuneki, Y., Morinaga, H., Liu, Y., 2009. New palaeomagnetic data supporting the extent of the stable body of the South China Block since the Cretaceous and some implications on magnetization acquisition of red beds. *Geophys. J. Int.* 178 (3), 1327–1336.
- Van der Voo, R., van Hinsbergen, D.J., Domeier, M., Spakman, W., Torsvik, H., 2015.

- Latest Jurassic–earliest Cretaceous closure of the Mongol-Okhotsk Ocean. In: Anderson, T.H., Didenko, A.N., Johnson, C., Khanchuk, A.I., MacDonald, J., Schwartz, J. (Eds.), Late Jurassic Margin of Laurasia - A Record of Faulting Accommodating Plate Rotation. Geological Society of America Special Paper 513. pp. 589–606.
- van Hinsbergen, D.J.J., Kapp, P., Dupont-Nivet, G., Lippert, P.C., DeCelles, P.G., Torsvik, T.H., 2011a. Restoration of Cenozoic deformation in Asia and the size of Greater India. *Tectonics* 30 (doi:5010.1029/2011TC002908).
- van Hinsbergen, D.J.J., Steinberger, B., Doubrovine, P.V., Gassmöller, R., 2011b. Acceleration and deceleration of India-Asia convergence since the Cretaceous: roles of mantle plumes and continental collision. *J. Geophys. Res.* 116 (B6), B06101. <http://dx.doi.org/10.1029/2010JB008051>.
- van Hinsbergen, D.J.J., Lippert, P.C., Dupont-Nivet, G., McQuarrie, N., Doubrovine, P.V., Spakman, W., Torsvik, T.H., 2012. Greater India Basin hypothesis and a two-stage Cenozoic collision between India and Asia. *Proc. Natl. Acad. Sci. U. S. A.* 109 (20), 7659–7664.
- Vigny, C., Socquet, A., Rangin, C., Chamot-Rooke, N., Pubellier, M., Bouin, M.N., Bertrand, G., Becker, M., 2003. Present-day crustal deformation around Sagaing fault, Myanmar. *J. Geophys. Res.* 108 (B11). <http://dx.doi.org/10.1029/2002JB001999>.
- Wang, E., Burchfiel, B.C., 1997. Interpretation of Cenozoic tectonics in the right-lateral accommodation zone between the Ailao Shan shear zone and the eastern Himalayan Syntaxis. *Int. Geol. Rev.* 39 (3), 191–219.
- Wang, B., Yang, Z., 2007. Late Cretaceous paleomagnetic results from southeastern China, and their geological implication. *Earth Planet. Sci. Lett.* 258 (1–2), 315–333.
- Wang, X., Yan, J., Lin, J., 1989. The inverted structure and its significance in petroleum geology. *Earth Sci. J. China Univ. Geosci.* 14 (1), 101–108.
- Wang, E., Burchfiel, B.C., Royden, L.H., Chen, L.Z., Chen, J.S., Li, W.X., Chen, Z.L., 1998a. Late Cenozoic Xianshuihe-Xiaojiang, Red River, and Dali fault systems of Southwestern Sichuan and Central Yunnan, China. *Geol. Soc. Am. Spec. Pap.* 327, 1–108.
- Wang, P.L., Lo, C.H., Lee, T.Y., Chung, S.L., Lan, C.Y., Yem, N.T., 1998b. Thermochronological evidence for the movement of the Ailao Shan Red River shear zone: a perspective from Vietnam. *Geology* 26 (10), 887–890.
- Wang, Y., Fan, W., Zhang, Y., Peng, T., Chen, X., Xu, Y., 2006. Kinematics and $^{40}\text{Ar}/^{39}\text{Ar}$ geochronology of the Gaoligong and Chongshan shear systems, western Yunnan, China: implications for early Oligocene tectonic extrusion of SE Asia. *Tectonophysics* 418 (3), 235–254.
- Wang, G., Wan, J., Wang, E., Zheng, D., Li, F., 2008a. Late Cenozoic to recent transtensional deformation across the southern part of the Gaoligong shear zone between the Indian plate and SE margin of the Tibetan plateau and its tectonic origin. *Tectonophysics* 460 (1–4), 1–20.
- Wang, S., Fan, C., Wang, G., Wang, E., 2008b. Late Cenozoic deformation along the northwestern continuation of the Xianshuihe fault system, Eastern Tibetan Plateau. *Geol. Soc. Am. Bull.* 120 (3–4), 312–327.
- Wang, S., Fang, X.M., Zheng, D.W., Wang, E.C., 2009. Initiation of slip along the Xianshuihe fault zone, eastern Tibet, constrained by K/Ar and fission-track ages. *Int. Geol. Rev.* 51 (12), 1121–1131.
- Wang, F., Yang, L.K., Wang, L., Shen, J.L., Xing, G.F., Chen, R., Pan, Y.X., Zhu, R.X., 2010a. The boundary ages of the late Mesozoic volcanic-sedimentary strata on South China: constrains from $^{40}\text{Ar}/^{39}\text{Ar}$ geochronology and paleomagnetism. *Science in China, Series D* 40 (11), 1552–1570.
- Wang, Y., Zhang, A., Fan, W., Peng, T., Zhang, F., Zhang, Y., Bi, X., 2010b. Petrogenesis of late Triassic post-collisional basaltic rocks of the Lancangjiang tectonic zone, southwest China, and tectonic implications for the evolution of the eastern Paleotethys: geochronological and geochemical constraints. *Lithos* 120 (3–4), 529–546.
- Wang, Y., Sieh, K., Tun, S.T., Lai, K.-Y., Myint, T., 2014. Active tectonics and earthquake potential of the Myanmar region. *J. Geophys. Res.* 119 (4), 3767–3822.
- Wang, H., Yang, Z., Tong, Y., Gao, L., Jing, X., Zhang, H., 2016. Palaeomagnetic results from palaeogene red beds of the Chuan-Dian Fragment, southeastern margin of the Tibetan Plateau: implications for the displacement on the Xianshuihe–Xiaojiang fault systems. *Int. Geol. Rev.* <http://dx.doi.org/10.1080/00206814.2016.1157710>.
- Wu, H., Zhang, L., Ji, S., 1989. The Red River-Ailaoshan fault zone—a Himalayan large sinistral strike-slip intracontinental shear zone. *Sci. Geol. Sin.* 1, 1–8.
- Wu, H., Boulter, C., Ke, B., Stow, D., Wang, Z., 1995. The Changning-Menglian suture zone; a segment of the major Cathaysian-Gondwana divide in Southeast Asia. *Tectonophysics* 242 (3), 267–280.
- Yamashita, I., Surinkum, A., Wada, Y., Fujihara, M., Yokoyama, M., Zaman, H., Otofujii, Y.-i., 2011. Paleomagnetism of the Middle-Late Jurassic to Cretaceous red beds from the Peninsular Thailand: implications for collision tectonics. *J. Asian Earth Sci.* 40 (3), 784–796.
- Yan, M., Voo, R.V.D., Tauxe, L., Fang, X., Parés, J.M., 2005. Shallow bias in Neogene palaeomagnetic directions from the Guide Basin, NE Tibet, caused by inclination error. *Geophys. J. Int.* 163 (3), 944–948.
- Yang, Z.Y., Besse, J., 1993. Paleomagnetic study of Permian and Mesozoic sedimentary rocks from Northern Thailand supports the extrusion model for Indochina. *Earth Planet. Sci. Lett.* 117 (3–4), 525–552.
- Yang, Z.Y., Besse, J., 2001c. New Mesozoic apparent polar wander path for south China: tectonic consequences. *J. Geophys. Res.* 106 (B5), 8493–8520.
- Yang, Z.Y., Besse, J., Suthetorn, V., Bassoulet, J.P., Fontaine, H., Buffetaut, E., 1995. Lower-Middle Jurassic paleomagnetic data from the Mae Sot area (Thailand): paleogeographic evolution and deformation history of southeastern Asia. *Earth Planet. Sci. Lett.* 136 (3–4), 325–341.
- Yang, Z.Y., Sun, Z.M., Ma, X.H., Yin, J.Y., Otofujii, Y., 2001a. Paleomagnetic study of the early Tertiary on both sides of the Red River and its geological implications. *Acta Geol. Sin.* 75 (1), 35–44 (In Chinese with English abstract).
- Yang, Z.Y., Yin, J.Y., Sun, Z.M., Otofujii, Y., Sato, K., 2001b. Discrepant Cretaceous paleomagnetic poles between Eastern China and Indochina: a consequence of the extrusion of Indochina. *Tectonophysics* 334 (2), 101–113.
- Yao, J., Shu, L., Santosh, M., Li, J., 2013. Geochronology and Hf isotope of detrital zircons from Precambrian sequences in the eastern Jiangnan Orogen: constraining the assembly of Yangtze and Cathaysia Blocks in South China. *J. Asian Earth Sci.* 74, 225–243.
- Yi, Z., Huang, B.C., Chen, J.S., Chen, L.W., Wang, H.L., 2011. Paleomagnetism of early Paleogene marine sediments in southern Tibet, China: implications for onset of the India-Asia collision and size of Greater India. *Earth Planet. Sci. Lett.* 309, 153–165.
- Yoshioka, S., Liu, Y., Sato, K., Inokuchi, H., Su, L., Zaman, H., Otofujii, Y., 2003. Paleomagnetic evidence for post-Cretaceous internal deformation of the Chuan Dian Fragment in the Yangtze block: a consequence of indentation of India into Asia. *Tectonophysics* 376 (1–2), 61–74.
- Zhang, L., Schärer, U., 1999. Age and origin of magmatism along the Cenozoic Red River shear belt, China. *Contrib. Mineral. Petrol.* 134 (1), 67–85.
- Zhang, Y.Q., Chen, W., Yang, N., 2004. Ar-40/Ar-39 dating of shear deformation of the Xianshuihe fault zone in west Sichuan and its tectonic significance. *Science in China, Series D* 47 (9), 794–803.
- Zhang, B., Zhang, J.J., Zhong, D.L., 2010. Structure, kinematics and ages of transpression during strain-partitioning in the Chongshan shear zone, western Yunnan, China. *J. Struct. Geol.* 32 (4), 445–463.
- Zhang, B., Zhang, J.J., Zhong, D.L., Yang, L.K., Yue, Y.H., Yan, S.Y., 2012a. Polystage deformation of the Gaoligong metamorphic zone: structures, Ar-40/Ar-39 mica ages, and tectonic implications. *J. Struct. Geol.* 37, 1–18.
- Zhao, X., Coe, R.S., 1987. Paleomagnetic constraints on the collision and rotation of North and South China. *Nature* 327, 141–144.
- Zhao, J., Huang, B., Yan, Y., Zhang, D., 2015. Late Triassic paleomagnetic result from the Baoshan Terrane, West Yunnan of China: implication for orientation of the East Paleotethys suture zone and timing of the Sibumasu-Indochina collision. *J. Asian Earth Sci.* 111, 350–364.
- Zhong, D.L., 1998. Paleo-Tethys Orogenic Belt in Western Yunnan-Sichuan. Science Press, Beijing (p231).
- Zhu, Z.M., Morinaga, H., Gui, R.J., Xu, S.Q., Liu, Y.Y., 2006. Paleomagnetic constraints on the extent of the stable body of the South China Block since the Cretaceous: new data from the Yuanma Basin, China. *Earth Planet. Sci. Lett.* 248 (1–2), 533–544.
- Zhu, R., Potts, R., Pan, Y.X., Lue, L.Q., Yao, H.T., Deng, C.L., Qin, H.F., 2008. Paleomagnetism of the Yuanmou Basin near the southeastern margin of the Tibetan Plateau and its constraints on late Neogene sedimentation and tectonic rotation. *Earth Planet. Sci. Lett.* 272 (1–2), 97–104.